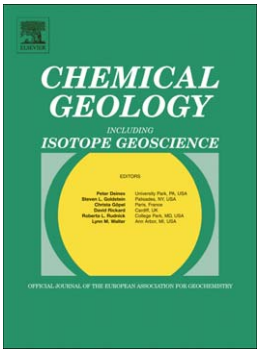

A stable (Li, O) and radiogenic (Sr, Nd) isotope perspective on metasomatic processes in a subducting slab

Ralf Halama, Timm John, Petra Herms, Folkmar Hauff, Volker Schenk

PII: S0009-2541(10)00433-X
DOI: doi: 10.1016/j.chemgeo.2010.12.001
Reference: CHEMGE 16106

To appear in: *Chemical Geology*

Received date: 21 April 2010
Revised date: 1 November 2010
Accepted date: 1 December 2010

Please cite this article as: Halama, Ralf, John, Timm, Herms, Petra, Hauff, Folkmar, Schenk, Volker, A stable (Li, O) and radiogenic (Sr, Nd) isotope perspective on metasomatic processes in a subducting slab, *Chemical Geology* (2010), doi: 10.1016/j.chemgeo.2010.12.001

A stable (Li, O) and radiogenic (Sr, Nd) isotope perspective on metasomatic processes in a subducting slab

Ralf Halama[a,b,*], Timm John[c], Petra Herms[a], Folkmar Hauff[d] and Volker Schenk[a]

[a] SFB 574 and Institut für Geowissenschaften, Universität Kiel, Ludewig-Meyn-Str. 10, 24118 Kiel, Germany

[b] Geochemistry Laboratory, Department of Geology, University of Maryland, College Park, MD 20742, USA

[c] Institut für Mineralogie, Universität Münster, Corrensstr. 24, 48149 Münster, Germany

[d] SFB 574 and IFM-GEOMAR, Wischhofstr. 1-3, 24148 Kiel, Germany

* Corresponding author contact information:
Ralf Halama
Institut für Geowissenschaften and SFB 574
Universität Kiel, 24098 Kiel, Germany
E-mail: *rh@min.uni-kiel.de*
Tel: +49-431-880-1911
Fax: +49-431-880-4457

Abstract

Two distinct types of eclogites from the Raspas Complex (Ecuador), which can be distinguished based on petrography and trace element geochemistry, were analyzed for their stable (Li, O) and radiogenic (Sr, Nd) isotope signature to constrain metasomatic changes due to fluid-overprinting in metabasaltic rocks at high-pressure conditions and to identify fluid sources. MORB-type eclogites are characterized by a relative LREE depletion similar to MORB. High-pressure (HP) minerals from this type of eclogite have highly variable oxygen isotope compositions (garnet: +4.1 to +9.8 ‰; omphacite: +6.1 to +11.0 ‰; phengite: 8.7 to 10.4 ‰; amphibole: 6.2 to 10.1 ‰) and generally show equilibrium oxygen isotope fractionation. Initial $^{87}Sr/^{86}Sr$ isotope ratios are also variable (0.7037-0.7063), whereas εNd_{130Ma} values (+8.3 to +11.0) are relatively similar. Sr and O isotopic compositional differences among rocks on outcrop scale, the preservation of O isotopic compositions of low-temperature altered oceanic crust, and Sr-Nd isotopic trends typical for seafloor alteration suggest inheritance from variably altered oceanic crust. However, decreasing δ^7Li values (-0.5 to -12.9 ‰) with increasing Li concentrations (11-94 ppm) indicate Li isotope fractionation by diffusion related to fluid-rock interaction. Li isotopes prove to be a very sensitive tracer of metasomatism, although the small effects on the Sr-Nd-O isotope systems suggest that the fluid-induced metasomatic event in the MORB-type eclogites was small-scale at low-water/rock ratios. This metasomatic fluid is thought to predominantly derive from in situ dehydration of MORB-type rocks.

Zoisite eclogites, the second eclogite type from the Raspas Complex, are characterized by the presence of zoisite and enrichment in many incompatible trace elements compared to the MORB-type eclogites. The zoisite eclogites have a homogenous Sr-Nd isotopic signature (Initial $^{87}Sr/^{86}Sr$ = 0.7075-0.7081, εNd_{130Ma} = -6.7 to -8.7), interpreted to reflect a metasomatic overprint. The isotopic signature can be attributed to the metasomatic formation of zoisite because associated zoisite veins are isotopically similar. Relatively homogenous O isotope values for garnet (10.9-12.3 ‰) omphacite (9.4 to 10.8 ‰), amphibole (10.0-10.1 ‰) and zoisite (10.5-11.9 ‰) and inter-mineral O isotopic disequilibria are consistent with a metasomatic overprint via open-system fluid input. Li concentrations (46-76 ppm) and δ^7Li values of the zoisite eclogites overlap the range of the MORB-type eclogites. The large amount of fluid required for isotopic homogenization, combined with the results from fluid inclusion studies, suggests that deserpentinization played a major role in generating the metasomatic fluid that altered the zoisite eclogites. However, influence of a (meta)sedimentary source is required based on Sr-Nd isotope data and trace element

enrichments. The significant geochemical variation in the various eclogites generated by interaction with metasomatic fluids has to be considered in attempts to constrain recycling at convergent margins.

Keywords: subduction, eclogite, metasomatism, seafloor alteration, lithium isotopes, Sr-Nd-O isotopes

1. INTRODUCTION

High-pressure metamorphic rocks represent natural probes into the subducting lithosphere and provide important information about pathways and processes of element cycling in subduction zones. The direct examination of subduction zone metamorphic rocks provides insight of how mass is redistributed during metamorphism (e.g., Bebout, 1991; Beinlich et al., 2010; Gao et al., 2007; John et al., 2008; King et al., 2004; Sorensen and Grossman, 1989; Spandler et al., 2003, 2004), about the nature of slab-derived agents added to arc lava sources and about chemical changes in subducting rocks potentially contributing to the geochemical heterogeneity of the upper mantle (e.g., Bebout, 2007; Breeding et al., 2004, John et al., 2004). Increasing attention has been directed towards metasomatic processes within subducted rocks because metasomatic rocks can constitute new bulk compositions that can influence the redistribution of major and trace elements (Bebout, 2007; King et al., 2006, 2007; Scambelluri et al., 2006; Zack and John, 2007). Metasomatic rocks can also affect the composition of slab fluids as they may contain mineral assemblages that are able to transport water to great depths in the subduction zone (e.g., Schmidt and Poli, 1998). Several studies have looked at the metasomatic overprint by slab-derived fluids/melts in the mantle wedge above the subducting slab (e.g., Halama et al., 2009; Paquin et al., 2004; Scambelluri et al., 2006; Zanetti et al., 1999), but the metasomatic effects within the lithospheric slab itself have been relatively little studied (e.g., Beinlich et al., 2010; Marschall et al., 2009; Molina et al., 2002). Fluids are important in catalyzing prograde metamorphic transformations, for instance during eclogitization processes (e.g., Austrheim, 1987; Putnis and John, 2010). Fluids in high-pressure (HP) metamorphic rocks also play a key role in promoting equilibration of isotopic systems used as geochronometers (Glodny et al., 2003). Multimineral isochrons record fluid-induced recrystallization events rather than stages of cooling because full isotopic homogenization is not achieved in rocks that remain devoid of fluids (Glodny et al., 2003, 2008). Without fluids, isotopic resetting is kinetically locked or restricted to sluggish intermineral diffusion. In general, the modification of pre-subduction isotopic compositions by fluid-rock interaction at HP conditions is a common feature (Bebout, 2007; Berger et al., 2010; King et al., 2006). During exhumation, HP subducted rocks can be incorporated into the subduction channel, i.e. the intensely serpentinized part of the mantle wedge above the surface of the subducted slab (e.g., Gerya et al., 2002), and re-hydration and addition of fluid-mobile elements from slab-derived fluids can be expected (Bebout, 1991; Horodyskyj et al.,

2009; Marschall et al., 2007a; Sorensen and Grossman, 1989; Sorensen et al., 1997; van der Straaten et al., 2008).

Lithium is mobile in hydrous fluids and there is a strong isotopic fractionation between its two stable isotopes at low temperatures due to the large relative mass difference (~16%) (Tomascak, 2004). Recent studies demonstrated that the Li isotope system is very sensitive to metasomatic enrichment processes (Marschall et al., 2009; Penniston-Dorland et al., 2010). A pioneering study by Zack et al. (2003) interpreted low δ^7Li values in orogenic eclogites as a result of Li isotopic fractionation during subduction dehydration, but the later investigation by Marschall et al. (2007b), which incorporated new experimental data, showed that Li isotope fractionation is most likely due to diffusion. Metamorphic dehydration of shales is similarly unable to shift Li isotope signatures significantly (Teng et al., 2007). Unlike oxygen, lithium has trace concentrations in most rocks and has therefore a differing sensitivity to fluid-rock interaction than the O isotope system, which is widely used to constrain the extent of fluid flow and to distinguish between external and internal fluid sources (e.g., Barnicoat and Cartwright, 1995; Bebout and Barton, 1993; Zheng et al., 2003). The Rb-Sr system has been applied to provide constraints on sources and nature of fluids at depth (e.g., Glodny et al., 2003), and Sr isotopes can indicate the presence of a metamorphic fluid in mélange rocks (King et al., 2006) or previous seafloor alteration (Miller et al., 1988). In contrast, Nd isotopes appear to behave more conservative (King et al., 2006).

The major aims of this study are to characterize the geochemical and isotopic imprint of slab-derived fluids responsible for metasomatic changes in eclogites at HP conditions and to gain insight into element redistribution by metasomatic processes within the subducting lithosphere. We investigate a suite of HP metamorphic rocks from the Raspas Complex, Ecuador, which comprises two distinct types of eclogites together with blueschists, serpentinized peridotites and metasedimentary rocks. This sample set has been the subject of several detailed studies in which petrology, major and trace element geochemistry, fluid inclusions and N isotopic compositions have been investigated and where several lines of evidence point toward metasomatic changes (John et al., 2010; Halama et al., 2010; Herms et al., submitted). In this study, we combine stable (Li, O) and radiogenic (Sr, Nd) isotope data with in situ trace element data to unravel the metasomatic effects on the various isotopic systems, which prove to be sensitive to distinct processes happening in the subducting slab.

2. GEOLOGY AND SAMPLE DESCRIPTION

2.1. Geological setting

The Raspas complex is a high-pressure metamorphic complex in the Andes of southwest Ecuador (Fig. 1) and constitutes the only known eclogite occurrence among the Andean HP rocks (Arculus et al., 1999; Feininger, 1980). It represents an exhumed terrane fragment of oceanic lithosphere (Arculus et al., 1999), which can be interpreted as a high-pressure ophiolite (John et al., 2010). The complex is subdivided into the Raspas Formation, which comprises eclogites, blueschists and metasediments, and the El Toro Formation, which consists of eclogite-facies, serpentinized peridotites (Feininger, 1980; Gabriele et al., 2003). Peak P-T conditions for eclogites and garnet-chloritoid-kyanite metapelites are very similar at about 2 GPa and 550-600°C (Gabriele et al., 2003; John et al., 2010). The partially serpentinized peridotites of the El Toro Formation locally host mafic dikes that have preserved eclogitic mineral assemblages, indicating subduction depths similar to those of the associated Raspas Formation (Gabriele, 2002). The age of metamorphism in the Raspas complex has been dated by Lu-Hf and gave overlapping ages of around 130 Ma for garnet growth in eclogites, blueschists and metapelites (John et al., 2010).

The eclogites of the Raspas complex can be subdivided into eclogites with geochemical signatures typical of mid-ocean ridge basalt (MORB) and zoisite eclogites that are enriched in rare earth elements (REE) compared to the MORB-type eclogites. In the isolated outcrops within the Quebrada Raspas, macroscopic differences were not identifiable, impeding clarification of contact relations. Whereas MORB-type eclogites are widespread, the occurrence of zoisite eclogites is spatially restricted to a canyon of the Rio Raspas ("Cañón Eclogita"; Feininger, 1978). The MORB-type eclogites are interpreted to represent former mid-ocean ridge oceanic crust (John et al., 2010). They have experienced seafloor alteration (Halama et al., 2010), were subsequently transformed into blueschists and eventually dehydrated to become eclogites. In contrast, formation of the zoisite eclogites is attributed to a fluid-induced HP metasomatic overprint. Sample locations, petrography and mineral chemistry of the samples analyzed in this study have been described in accompanying studies (Halama et al., 2010; Herms et al., submitted; John et al., 2010), so that key features are only briefly summarized here.

2.2. MORB-type eclogites and amphibole eclogite

Major mineral phases in the MORB-type eclogites are garnet + omphacite + rutile + amphibole ± quartz ± phengite. Accessory phases include rutile, quartz, phengite, carbonate

and clinozoisite. The MORB-type eclogites are fine- to medium-grained, banded rocks with a stretching lineation defined by omphacite. Garnets occur as euhedral, zoned pophyroblasts with Fe-rich cores (X_{Fe} = 0.76-0.82; $Alm_{58-56}Pyr_{13-16}Sps_{2-4}Grs_{27-24}$) and less Fe-rich rims (X_{Fe} = 0.68-0.73; $Alm_{52-54}Pyr_{24-19}Sps_{1}Grs_{23-26}$). All minerals of the matrix can occur as inclusions in garnet, whereby omphacite is present only in garnet rims. Omphacite has a quite uniform composition (37-43 mol% jadeite (Jd) component) and is in textural equilibrium with Mg-katophoritic to barroisitic amphibole. One sample (SEC 50-1) is retrogressed based on the occurrence of paragonite and barroisitic amphibole similar in composition to sodic-calcic amphiboles in associated blueschists. Geochemically, the MORB-type eclogites are basaltic (44-50 wt.% SiO_2) with LREE-depleted (La_N/Yb_N = 0.49-0.72) chondrite-normalized REE patterns and trace element ratios used for fingerprinting basalts (Hf/Yb, Nb/Zr, Th/Yb, TiO_2/Yb) that overlap with values for N-MORB (John et al., 2010).

The main minerals of the amphibole eclogite (sample SEC 13-1) are garnet and amphibole, whereas omphacite (35 mol% Jd component) only occurs as inclusions in amphibole. Compositionally, amphibole can be classified as magnesiohornblende or barroisite. Garnet shows limited compositional variability ($Alm_{57-48}Pyr_{19-24}Sps_{1}Grs_{23-27}$) with prograde zoning. Accessory minerals are rutile and quartz. The amphibole eclogite has HREE contents and immobile trace element ratios similar to the MORB-type eclogites, but it is relatively enriched in Fe_2O_3, whereas CaO, Na_2O and SiO_2 as well light and middle REE are depleted. The amount of amphibole appears to be related to the amount of fluid available during the prograde metamorphic evolution (John et al., 2010).

2.3. Zoisite eclogites and zoisite vein

Zoisite eclogites are characterized by subhedral to anhedral zoisite as major mineral constituent (5-20 vol.%). Zoisite veins of mm- to dm-thickness are always spatially close to the zoisite eclogites on outcrop scale and cut the schistosity of the eclogites discordantly. Garnet porphyroblasts show an overall prograde zoning with Fe-rich cores (X_{Fe} = 0.85-0.93; $Alm_{69-65}Pyr_{6-10}Sps_{5-2}Grs_{20-23}$) and Mg-rich rims ($X_{Fe}$ = 0.79-0.84; $Alm_{56-63}Pyr_{14-8}Sps_{1-2}Grs_{29-26}$). Mineral inclusions in garnet include rutile, albite, calcite, quartz and graphite in the cores and omphacite, rutile, zoisite/clinozoisite and hornblende in the rims. Omphacite (Jd = 31-45 mol%) is strongly deformed and partly recrystallized. Zoisite forms elongated blasts of similar grain size as garnet and omphacite. In terms of whole-rock geochemistry, the zoisite eclogites are basaltic (45.2 – 48.5 wt.% SiO_2) and enriched in Th, U, LREE and high field strength elements (HFSE) relative to the MORB-type eclogites (Halama et al., 2010).

Chondrite-normalized REE patterns show negative slopes (La_N/Yb_N = 7.1-8.8) and small negative Eu anomalies.

Zoisite veins are nearly monomineralic (> 90 vol.% zoisite) with accessory albite and titanite. In some parts of the broader veins, euhedral zoisite crystals and interstitial albite indicate growth in an open space. In the deformed parts of the zoisite veins, thin veinlets containing albite and Ba-rich K-feldspar as well as calcite veins are found. These can be related to repeated activation of the vein. Whole-rock vein compositions are characterized by low SiO_2 (41-44 wt.%), MgO (0.2-0.3 wt.%), Na_2O (0.5-1.5 wt.%) and K_2O contents (0.3-1.2 wt.%), whereas Al_2O_3 (28-31 wt.%) and CaO (20-22 wt.%) contents are high, reflecting the almost monomineralic character. LREE concentrations are slightly higher than in the zoisite eclogites, but HREE are even more strongly depleted relative to the LREE (Halama et al., 2010), resulting in a highly fractionated pattern (La_N/Yb_N = 154). Strontium, U and Pb show the most prominent relative enrichments in normalized trace element diagrams. Compared to zoisite pegmatites derived from high-P melting of eclogite (Liebscher et al., 2007), several lines of evidence point towards a fluid origin for the Raspas zoisite veins: Relatively low peak P-T conditions with ~600°C at 1.8 GPa (vs. 680-750°C at 2.3-3.1 GPa for the zoisite pegmatites) and the essentially monomineralic character (vs. the occurrence of zoisite in a plagioclase-quartz matrix with amphibole). Significant geochemical differences to zoisite pegmatites (Liebscher et al., 2007) and sediment melts (Johnson and Plank, 1999), such as low SiO_2, low Na_2O and high CaO contents, also support a fluid origin of the veins.

2.4. Associated blueschists, metasedimentary rocks and peridotites

Rocks associated with the eclogites in the Raspas complex were investigated to evaluate their geochemical relationship to the eclogites and to potential metasomatic agents. Blueschists contain bluish amphibole with greenish- to brownish cores, garnet, clinozoisite, omphacite, paragonite, phengite, quartz, titanite and rutile. They have trace element characteristics suggesting an affinity to seamounts (John et al., 2010). The metasedimentary rocks are graphite-bearing garnet mica-schists interpreted as dominantly terrigenous sediments deposited at the Andean continental margin and incorporated into an accretionary prism (Bosch et al., 2002), but less silicic, metavolcanic schists also occur. The peridotites from the El Toro formation are serpentinized to variable degrees (≤ 10 to 95%). They contain antigorite, chlorite, amphibole, spinel (chromite and magnetite), titanian clinohumite, carbonate and chrysotile. In less serpentinized rocks, primary olivine, orthopyroxene and

clinopyroxene may be preserved. Geochemically, they resemble depleted mantle (John et al., 2010).

3. Analytical methods

3.1. *In situ* trace element analyses

In situ trace element analyses of minerals were carried out at the University of Würzburg using a 266 nm Merchatek LUV 266x laser coupled to a single collector quadrupole Agilent 7500c ICP-MS. Spot analyses were applied with a laser repetition rate of 10 Hz and an energy of 0.36-0.54 mJ. The laser spot size on the sample surface was ~40 μm. SiO_2, determined by electron microprobe, was used as internal standard element (see supplementary material for representative microprobe analyses). Differences in SiO_2 contents within and between individual silicate minerals are small, so that the error introduced from the microprobe analysis of SiO_2 can be neglected relative to the error related to the laser ICP-MS measurement. Nevertheless, for each sample, an average SiO_2 content of garnet cores and rims was calculated for internal standardization. For instance, garnet core and rim compositions gave 37.4 vs. 37.7 wt.% SiO_2 in sample SEC 27-2 and 37.0 vs. 38.2 wt.% SiO_2 in sample SEC 29-2. For the time-resolved laser ablation, NIST 612 glass was used for instrument calibration and NIST 610 and NIST 614 were used as secondary standards (Pearce et al., 1997). Reproducibility, accuracy and precision of the method were controlled by repeated analyses of the NIST standards, with a precision usually better than 10% (see Schulz et al. (2006) for details). Signal quantification was conducted using the Glitter Version 3.0 Online Interactive Data Reduction for LA-ICP-MS Program (Macquarie Research Ltd.). Some of the in situ trace element data, focusing on zoisite and omphacite, are published in an accompanying paper (Herms et al., submitted), and hence we concentrate in this study on trace element contents in garnet and, in particular, on Li in the various minerals.

3.2. Oxygen isotopic analyses

The oxygen isotope composition of handpicked and ultrasonically cleaned mineral separates was measured using a laser fluorination method similar to that described by Sharp (1990). Details about the analytical protocol and the mass spectrometric measurements can be found in Pack et al. (2007). In brief, samples are fluorinated using a 50 W CO_2 laser and purified F_2 gas. The extracted O_2 is trapped on a 5Å molecular sieve. Analyses of O_2 gas were

carried out using a conventional dual inlet system of a Finnigan Delta plus mass spectrometer. Results are reported as the per mil deviation from Vienna Standard Mean Ocean Water (V-SMOW) in the standard δ-notation. Measurements of the UWG-2 garnet reference material gave $\delta^{18}O = 5.66 \pm 0.08$ ‰ (1σ, n=9), in good agreement with the reference value of + 5.74 ± 0.15 ‰ given by Valley et al. (1995). Based on long-term reproducibility, an analytical uncertainty of ±0.2 ‰ is assumed for the samples analyzed in this study.

3.3. Strontium and neodymium isotopic analyses

Sr and Nd isotopic analyses used sample solutions from ICP-MS trace element measurements (see John et al. (2008) for details of the dissolution procedures) by sequential evaporation of the ca 50ml diluted HNO_3 solution and conversion of the sample matrix into chloride form. The ion exchange procedures followed those described in Hoernle and Tilton (1991). Isotopic ratios were determined in static multi-collection on a Finnigan MAT262 (Sr) and a Thermo-Finnigan TRITON (Nd) thermal ionization mass spectrometer (TIMS) at IFM-GEOMAR in Kiel, Germany. Sr and Nd isotopic ratios are normalized within run to $^{86}Sr/^{84}Sr = 0.1194$ and $^{146}Nd/^{144}Nd = 0.7219$. Analyses of reference materials along with the samples gave $^{87}Sr/^{86}Sr = 0.710196 \pm 0.000019$ (2σ, n=5) for NBS-987 and $^{143}Nd/^{144}Nd = 0.511846 \pm 0.000007$ (2σ, n=7) for La Jolla. Sample data are corrected for the offset from the accepted values (0.710250 for NBS-987 and 0.511850 for La Jolla). Total chemistry blanks were < 100 pg for Sr and Nd and are thus considered negligible.

3.4. Lithium isotopic analyses

For Li isotopic analyses, samples were initially dissolved in a HF-HNO_3 mixture. Detailed procedures for sample dissolution and column chemistry are reported in Rudnick et al. (2004). After purification of Li on a cation exchange resin (Bio-Rad AG50w-X12), Li isotopic measurements were carried out using a Nu Plasma MC-ICP-MS at the University of Maryland. Details of the instrumental analysis are given by Teng et al. (2004). Each sample analysis is bracketed by measurements of the L-SVEC standard and the δ^7Li value of the sample is calculated relative to the average of the two bracketing L-SVEC runs. Two standard solutions, IRMM-016 (Qi et al., 1997) and the in-house UMD-1 standard (a purified Li solution from Alfa Aesar®) were routinely analyzed during the course of each analytical session. Results for both (IRMM-016: $\delta^7Li = +0.2 \pm 0.4$ ‰ (2σ, n=6); UMD-1: $\delta^7Li = +54.9 \pm 0.8$ ‰ (2σ, n=7) agree well with previously published data (e.g. Halama et al., 2007, 2008;

Rudnick et al. 2004). Two international reference materials were analyzed during the course of this study to evaluate the accuracy of the measurements. Basalt BHVO-1 gave δ^7Li = 4.6 ± 1.0 ‰ (2σ, n=4) and muscovite-quartz schist SDC-1 gave δ^7Li = 2.0 ± 0.9 ‰ (2σ, n=6 with two different dissolutions). The external precision of Li isotopic analyses, based on 2σ of repeat runs of pure Li standard solutions and rock solutions over a four-year period, is ≤ ± 1.0 ‰ (Teng et al., 2004, 2007).

4. Results

4.1. Li concentrations in minerals and zoning of REE and Li in garnet

Representative trace element analyses of garnets from Raspas eclogites are given in Table 1, and typical chondrite-normalized REE diagrams of garnet cores and rims as well as Li concentrations data from garnet, omphacite and amphibole are presented in Figs. 2-4. Garnets from both the MORB-type eclogites and the zoisite eclogites have very similar REE concentrations and patterns. LREE are typically below the detection limit and the REE patterns from Sm to Lu are distinct for garnet cores and rims (Fig. 2). Cores exhibit a smooth increase towards the HREE with Yb and Lu contents > 100 times chondrite. Rims have a hump in their pattern due to a steep increase from Sm to Tb, Dy or Ho, followed by a slight decrease towards Lu. Decreasing HREE concentrations from garnet cores to rims correlate with decreasing Sc, Ti and Y contents as well as with decreasing X_{Fe} values.

Lithium contents in garnets from MORB-type eclogites (typically 1-8 ppm Li) are on average lower than in those from zoisite eclogites, where cores have up to 30 ppm Li (Fig. 3). Large garnet porphyroblasts (> 1 mm) in the zoisite eclogites consistently show decreasing Li contents from core to rim that correlate with decreasing X_{Fe} values and HREE contents (Fig. 4). Omphacite is the main carrier of Li in all eclogites, but Li contents can vary significantly from sample to sample. Two of the MORB-type eclogites have omphacite with ~ 100 ppm Li, whereas in one sample (SEC 46-1), omphacite with only about 20 ppm Li occurs and another one (SEC 13-4) contains omphacite with 160-240 ppm Li (Fig. 3). Lithium concentrations in omphacite from the zoisite eclogites are more homogeneous and sample averages vary from 160 to 180 ppm. Compared to omphacite, amphiboles have relatively low Li contents (15-70 ppm), except for the amphibole eclogite, where amphibole is the main carrier of Li (71-84 ppm) due to the lack of omphacite.

4.2. Oxygen isotope compositions of mineral separates

Oxygen isotope data for mineral separates are presented in Table 2 and shown in Fig. 5. In MORB-type eclogites, $\delta^{18}O$ values of high-pressure minerals are highly variable: 4.1–9.8 ‰ for garnet, 6.1–11.0 ‰ for omphacite, 6.2–10.1 ‰ for amphibole and 9.6–10.4 ‰ for phengite. $\delta^{18}O$ values of the minerals from the blueschist (sample SEC 16-1) are within the range observed in the MORB-type eclogites. The relatively high $\delta^{18}O$ values of the constituent minerals, except for sample SEC 46-1, mean that O isotope compositions of whole-rock high-pressure metabasalts would be roughly in the range from 7 to 11 ‰, which is considerably higher than the value for fresh MORB glass (5.4–5.8 ‰; Eiler et al., 2000). In the zoisite eclogites, $\delta^{18}O$ values of garnet (10.9–12.3 ‰), omphacite (9.4–10.8 ‰), amphibole (10.0–10.1 ‰) and zoisite (10.5–11.9 ‰) show much less variability from sample to sample than the minerals of the MORB-type eclogites. Garnet is always isotopically heavier than both omphacite and amphibole, opposite to what is observed in the MORB-type eclogites. Moreover, garnet from the zoisite eclogites is always higher in $\delta^{18}O$ than garnet from the MORB-type eclogites, whereas values for omphacite and amphibole from the different eclogite types overlap. Zoisite from the zoisite vein ($\delta^{18}O$ = 11.8-12.1 ‰) is similar in O isotope composition to zoisite from the eclogites.

4.3. Sr and Nd isotope compositions

Rubidium, Sr, Sm and Nd concentrations and Rb-Sr and Sm-Nd isotopic compositions are shown in Table 3 and Fig. 6. MORB-type eclogites have high positive and relatively constant $\varepsilon Nd_{(T=130\ Ma)}$ values (+8.3 to +10.8), but more variable $Sr_{initial}$ isotopic compositions ($^{87}Sr/^{86}Sr_{(i)}$ = 0.7037-0.7063). On the Sr-Nd isotope diagram, they follow a trend with a slightly negative slope, starting from near the composition of the depleted mantle (DM) toward the amphibole eclogite. The zoisite eclogites, in contrast, show a very small range in $^{87}Sr/^{86}Sr_{(i)}$ values (0.7075-0.7081) and also little variation in $\varepsilon Nd_{(T=130\ Ma)}$ values (-8.7 to -6.7). Notably, their Sr-Nd isotopic compositions are very different from those of the MORB-type eclogites, but similar to the zoisite vein ($\varepsilon Nd_{(T=130\ Ma)}$ = -7.2). The blueschists overlap the MORB-type eclogites in terms of Sr isotopic composition, but they are characterized by distinctly lower $\varepsilon Nd_{(T=130\ Ma)}$ values of around +5.5. The two analyzed metapelites have high but variable $^{87}Sr/^{86}Sr_{(i)}$ (0.7073 and 0.7120) and negative $\varepsilon Nd_{(T=130\ Ma)}$ values (-1.6 and -7.1), which are somewhat less radiogenic than metapelites analyzed by Bosch et al. (2002).

4.4. Lithium whole-rock concentrations and isotope compositions

Lithium concentration and isotope data are summarized in Table 4. Lithium concentrations in the MORB-type eclogites vary from 11-94 ppm, whereas the zoisite eclogites show a smaller variation from 46 to 76 ppm Li. Li isotopic compositions of the eclogites are highly variable and range from -13 to 0, within the range observed for global orogenic eclogites (δ^7Li = -22 to +6; Marschall et al., 2007b), but lower than what is observed for MORB (δ^7Li = +1.6 to +5.6; Tomascak et al., 2008). The zoisite eclogites have δ^7Li values in the middle of the overall range for the eclogites. In contrast to the eclogites, the blueschists (19-63 ppm Li) have positive δ^7Li values (0 to +3). The serpentinized peridotites have low Li contents (<4 ppm) and also positive δ^7Li values (0 to +5). Li isotope compositions of the metapelites fall close to the average of upper continental crust (0 ± 2; Teng et al., 2004) and their Li contents range from 9 to 23 ppm.

For three samples, one MORB-type eclogite, the amphibole eclogite and one blueschist, Li isotopic compositions of separated minerals were analyzed (Table 4). All samples show apparent Li isotope disequilibria among coexisting minerals. In the MORB-type eclogite (sample SEC 43-1), $\Delta^7Li_{garnet\text{-}omphacite}$ (= $\delta^7Li_{garnet} - \delta^7Li_{omphacite}$) is +3.2, whereas $\Delta^7Li_{garnet\text{-}amphibole}$ in the amphibole eclogite (sample SEC 13-1) is -2.3. In the blueschist, $\Delta^7Li_{garnet\text{-}glaucophane}$ is +4.1.

5. Discussion

5.1. MORB-type eclogites: Evidence for seafloor alteration

The observed isotopic compositional variations in the MORB-type eclogites may, in principle, be caused by primary protolith heterogeneity, differences in the intensity of hydrothermal alteration of the oceanic crust, metasomatism in the subduction zone, heterogeneous overprinting by fluids during exhumation or low-T secondary alteration (e.g. Barnicoat and Cartwright, 1995; Bebout, 2007; Zheng et al., 2003). Since chondrite-normalized REE patterns and initial Nd isotopic ratios are very similar for the MORB-type eclogites, primary protolith heterogeneity is considered unlikely. Both retrograde overprinting and late stage, exhumation-related low-T alteration can be excluded based on the lack of textural evidence and because the major mineral phases (garnet (grt), omphacite (omp), amphibole, phengite (phe)) are in or near elemental and isotopic equilibrium. For instance,

three MORB-type eclogites (samples SEC 13-4, 42-6 and 43-1) have $D^{Li}_{grt(rim)-omp}$ values of 0.014 to 0.031, overlapping the range for high-pressure Li equilibrium distribution (0.018-0.043; Marschall et al., 2006). Within analytical error, all MORB-type eclogites have $\Delta^{18}O_{omp-grt}$ in the range 0-2 ‰ (Fig. 5), indicating O isotopic equilibration based on the approximate limits of equilibrium fractionation between omphacite and garnet at eclogite-facies conditions (Zheng et al., 2003). Three of four MORB-type eclogites samples (SEC 43-1, 44-1 and 47-1) have $\Delta^{18}O_{phe-grt}$ between +1.2 and +1.4, also consistent with equilibrium fractionation at eclogite-facies conditions, which should be between +1.2 and +2.1 at temperatures from 500 to 800°C based on calculations using the modified increment method (Zheng, 1993a, 1993b). Deviations in omphacite-garnet O isotope thermometry from peak-metamorphic temperatures may be related to temperature changes during garnet growth, which would make high spatial resolution data necessary to obtain reliable temperature estimates (Wiechert et al., 2002). In addition to the elemental and isotopic equilibration, REE patterns in garnet show prograde metamorphic growth with no indication for late disturbances (Fig. 2). HREE, which are compatible in garnet, are highly enriched in the cores, but have lower concentrations in the rims due to preferential HREE incorporation in the cores that grew earlier.

Oxygen isotope signatures of ocean-floor basalts are generally preserved through subduction-zone metamorphism, although $\delta^{18}O$ can locally be modified (e.g., Barnicoat and Cartwright, 1995). Devolatilization of subducting rocks is not considered to produce appreciable shifts in the O isotope composition because the majority of the O reservoir is retained in the residue (Bebout, 2007), and prograde metamorphic effects are thought not to lower $\delta^{18}O$ of a rock by more than 1-2 ‰ (Valley, 1986). The O isotope composition of the constituent minerals of the MORB-type eclogites falls into the range typically observed for low-temperature altered oceanic crust (Fig. 5). Very similar values in $\delta^{18}O$ for garnet (+9.2 to +11.5 ‰) and omphacite (+10.2 to +12.8 ‰) were observed in HP mafic rocks from Greece and interpreted as the result of low-T alteration by seawater (Putlitz et al., 2000). The seafloor-altered basalts are enriched in ^{18}O due to large positive O isotopic fractionation between clay minerals and water (Miller et al., 1988). Inheritance from pre-subduction basaltic precursors was also invoked to explain a large range in $\delta^{18}O$ of garnet (-4.6 to +6.0 ‰) from eclogites in the Dabie and Sulu terranes, China (Yui et al., 1997). As garnet is the most resistant mineral among the HP minerals to isotopic exchange during cooling (Gregory and Criss, 1986) and prograde variations in $\delta^{18}O$ in garnet are relatively small (< 1 ‰; e.g., Wiechert et al., 2002), it is concluded that the O isotope variations in minerals of the MORB-type eclogites reflect the effects of variable pre-subduction seafloor alteration. This is in

agreement with certain correlations between trace elements and trace element ratios in these rocks that follow seafloor alteration trends (e.g. Nb/U vs. U; Halama et al., 2010).

Additional support for a pre-subduction seafloor alteration in the MORB-type eclogites comes from Sr isotopes. The trend on the Sr-Nd isotope diagram is different from the mantle array, and the Sr isotope ratios appear to be shifted to higher values (Fig. 6), which reflects the effects expected from seafloor alteration (Staudigel et al., 1981). The amphibole eclogite with the most radiogenic Sr isotope composition is likely to have suffered the most intense alteration. Seafloor alteration accompanied by Sr isotope exchange (McCulloch et al., 1981) was also the preferred interpretation to explain a wide range in Sr isotopic values in studies on eclogites from the Eastern Alps (Miller et al., 1988) and metabasalts from the Franciscan complex (Nelson, 1995). A weak correlation (not shown) of O and Sr isotopes in the MORB-type eclogites confirms that seafloor alteration was an important process in the history of these rocks.

5.2. MORB-type eclogites: Internal Li metasomatism at HP conditions

Enrichment of Li in metamorphic rocks is a sensitive tracer of metasomatic processes (Marschall et al., 2009; Penniston-Dorland et al., 2010) and a comparison of the Raspas eclogites with submarine basalts can yield insights into fluid-rock interaction and Li mobility during subduction. The Li abundances in some of the MORB-type eclogites (11-94 ppm) are higher than the majority of published values for Li in igneous oceanic rocks. For instance, fresh oceanic crust has 3-8 ppm Li (Niu and Batiza, 1997), altered oceanic crust 1-35 ppm Li (Chan et al., 2002) and differentiated oceanic crust 10-30 ppm Li (Ryan and Langmuir, 1987). Lithium enrichment is also evident from a plot of Li/Dy versus Hf/Yb (Fig. 7a), where Dy is used as an element with an incompatibility similar to Li (Ryan and Langmuir, 1987) to eliminate effects of magmatic processes such as fractional crystallization, and Hf/Yb is used as a proxy for mantle source characteristics (John et al., 2004). There is a clear Li enrichment compared to fresh MORB, and many of the MORB-type eclogites have Li/Dy ratios significantly higher than typical AOC as well. These features suggest addition of Li after the onset of subduction, during eclogitization or exhumation. Lithium addition has not only been suggested for eclogites and other HP rocks, where it seems to be a common feature (Marschall et al., 2007b; Penniston-Dorland et al., 2010; Simons et al., 2010), but also in peridotites in a supra-subduction zone setting (Paquin et al., 2004), indicating a high Li mobility in deep subduction zone environments.

Lithium isotopic compositions of the MORB-type eclogites do not correlate with Sr isotope values, suggesting that the δ^7Li values are not inherited from seafloor alteration (Fig. 7b). If an alteration δ^7Li signal from AOC had been retained in the eclogites, one would expect that rocks with high Li contents show the most positive δ^7Li values (Chan et al., 1992; Marschall et al., 2007b). However, there is no indication of positive correlation between Li concentrations and δ^7Li in the MORB-type eclogites, suggesting that the Li isotopic signature was acquired due to metasomatic processes during subduction (Fig. 7c). Fresh and altered oceanic crust generally has positive δ^7Li values (e.g. Chan et al., 1992, 2002), and dehydration causes only small changes in Li isotope ratios in subducting crust (Marschall et al., 2007b). A simple Rayleigh distillation model (Fig. 7c) demonstrates that dehydration alone cannot account for δ^7Li values <0 ‰, in agreement with a more complex incremental dehydration model, which incorporates the temperature-dependence of partition coefficients and fractionation factors (Marschall et al., 2007b). Therefore, the light δ^7Li values of the Raspas MORB-type eclogites can best be explained by kinetic isotope fractionation during diffusive transport of Li through the eclogite body. This process produces low δ^7Li in the rock into which Li is diffusing from the fluid due to the higher diffusivity of the light ^{6}Li isotope (Richter et al., 2003). The elevated Li concentrations and the related low δ^7Li values may be explained by the diffusive transport in an internal fluid or could result from external fluids, in either case demonstrating a relatively high mobility of Li. However, the large range in whole-rock Li concentrations and differences in Li content of omphacite between the different samples (Fig. 3) exclude a long-termed connectivity of the fluid system and point to fluid flow dominantly along grain boundaries. These characteristics are interpreted to reflect the effects of spatially restricted, non-penetrative metasomatism in the MORB-type eclogites.

Lithium isotope fractionation between co-existing minerals can be used to evaluate Li isotope equilibria. For instance, inter-mineral isotopic variations in granulite xenoliths were related to diffusion-driven isotope fractionation (Teng et al., 2008) based on the large difference in diffusion rates between Li isotopes (Richter et al., 2003). In the Raspas eclogites, Li substitutes for Mg in 6-fold coordination in omphacite (Wunder et al., 2006), whereas Li can also occupy the M4(B)-site in 5-fold coordination in amphiboles (Wenger and Armbruster, 1991). For garnet, Li substitution mechanisms are difficult to confirm (Hanrahan et al., 2009). The correlation between Yb^{3+} and Li^{+} in individual garnets (Fig. 4) suggests that Li may replace HREE and Y, which occupy the 8-fold coordinated site (Meagher, 1982). Li would also occupy the 8-fold coordinated site if it substitutes for Mg, as in other Fe-Mg silicates (Wunder et al., 2006). Then, for equilibrium fractionation, the Li isotopic signature in

garnet should be lighter than in omphacite because the lighter isotope prefers the more highly coordinated site with the lower bond energy. The positive $\Delta^7Li_{garnet\text{-}omphacite}$ of the MORB-type eclogite can therefore be interpreted as a disequilibrium feature. In any case, the samples analyzed vary unsystematically in their inter-mineral fractionation factors. Garnet – omphacite pairs from Guatemalan eclogites similarly gave non-systematic Li isotopic differences ($\Delta^7Li_{garnet\text{-}omphacite}$ = -5.3 to +1.6; Simons et al., 2010). Clearly, Li isotope disequilibria are recorded in at least some of the HP rocks, which can be explained by kinetic Li isotope fractionation. Hence, the unsystematic differences observed for Li isotope fractionation between coexisting garnet and omphacite/amphibole suggest inter-mineral Li isotope disequilibria, which support the idea of diffusion-driven isotope fractionation.

Whereas Li concentrations and Li isotopes prove their potential as sensitive tracer of metasomatic processes in HP metabasaltic rocks, differences in O compositions reflect the effects of seafloor alteration. The preservation of large variations in $\delta^{18}O$ within otherwise geochemically similar rock types suggests that the fluid-rock interaction was relatively localized on grain boundaries or restricted to soluble, i.e. reactive minerals, as pervasive fluid infiltration with a high flux would tend to homogenize O isotopic ratios (e.g., Philippot et al., 2007; Zheng et al., 2002) if the minerals react with the fluid (Glodny et al., 2003; Putnis and John, 2010). The inherited differences in initial Sr isotopic compositions point to local derivation of the fluid or restricted fluid-mineral reactions, but argue against a large single fluid reservoir and intense fluid-rock interaction (Glodny et al., 2003). Moreover, no reasonable Rb-Sr and Sm-Nd isochrons can be obtained for the MORB-type eclogites. This demonstrates the lack of Sr and Nd isotope equilibration during eclogite-facies recrystallization on outcrop scale and is consistent with a non-pervasive metasomatic event. MORB-like Nd isotopic signatures and whole-rock REE patterns argue against an exotic fluid component and point towards a local fluid source. Only the highly mobile and fast diffusing Li, which diffuses 2-3 orders of magnitude faster than most other elements (Richter et al., 2003) and which is enriched in the fluid relative to the rock (e.g. Marschall et al., 2007a), was able to leave a geochemical imprint of the high-pressure fluid flow in the surrounding rocks. Consequently, the fluid release during the conversion of blueschist-facies metabasalts, representing altered and hydrated oceanic crust, to almost dry eclogite, here represented by the Raspas MORB-type eclogites, leads to low fluid fluxes at the site of dehydration and thus to a minor element mobility potential for isotope homogenization (e.g., Spandler et al., 2003). The fluid phase may occur as little as a layer of OH molecules in the grain boundary network of UHP rocks (e.g., Zheng et al., 2002). Moreover, the released fluids are at or near

equilibrium with the dehydrating host rocks and relatively diluted (Manning, 2004), further limiting the potential for chemical changes. Only where these fluids become channelized and higher fluxes will be reached more significant chemical feedback is to be expected (Spandler and Hermann, 2006; Zack and John, 2007).

5.3. Zoisite eclogites: Fluid infiltration and external metasomatic effects

The ubiquitous presence of zoisite, the occurrence of fluid inclusions in garnet, omphacite and zoisite, the association with zoisite veins and bulk rock enrichment in LREE and other trace elements (Pb, Sr, Th, U, Nb, Ta, Zr, Hf) indicates that the zoisite eclogites have experienced a pervasive metasomatic enrichment. Although REE and HFSE are often considered as relatively immobile, fluid-mobility of these elements has been described in several cases (e.g., Gao et al., 2007; Gieré and Williams, 1992). Geochemical similarities of the zoisite eclogites with the zoisite vein, such as similar Sr-Nd isotope compositions and relative enrichments in Pb, Sr, Th, U and LREE, are evidence that the zoisite eclogites truly reflect metasomatic changes related to fluid flow in the veins. They do not represent a distinct protolith like the Raspas blueschists, which have geochemical affinities to seamounts (John et al., 2010). The metasomatic enrichment in the zoisite eclogites overprinted any difference in protolith geochemistry to the MORB-type eclogites that may or may not have existed prior to subduction.

Diagrams using trace element concentrations and ratios that are used to distinguish between seafloor alteration and HP metasomatism (Bebout 2007), such as Nb/U vs. U, Th/U vs. Th and Ce/Pb vs. 1/Pb, clearly show that the MORB-type eclogites and the zoisite eclogites plot in different areas and exhibit distinct trends (Halama et al., 2010). There are no samples bridging the compositional gaps between the two types, suggesting that the distinct metasomatic overprints are not related to varying degrees of one event. Instead, the trace element data demonstrate that two distinct phases of metasomatism are required. The metasomatic trend seen in the zoisite eclogites is also distinct to seafloor alteration trends.

There are several lines of evidence that the zoisite eclogite metasomatism took place during eclogite-facies conditions. First, garnets in the zoisite eclogites have zoning patterns consistent with prograde metamorphic growth, indicated by high X_{Fe}, high Sc and HREE contents in the cores compared to the rims (Figs. 2 and 4). Second, garnet rims are in Li elemental equilibrium with omphacite, as shown by the overlap of $D^{Li}_{grt(rim)\text{-}omp}$ values (0.033-0.061) with published equilibrium distribution values ($D_{grt\text{-}omp}$ around 0.03; Marschall

et al., 2006). Lithium is enriched in the garnet cores relative to the rims, indicating a prograde growth-zoning pattern for Li with decreasing Li contents towards the rims (Fig. 4). This is surprising as Li is usually considered relatively incompatible in garnet, with Li partition coefficients $D_{grt\text{-}fluid}$ in the range 0.005-0.008 (Brenan et al., 1998; Marschall et al., 2007a). A plausible explanation for the Li decrease during prograde garnet growth is a coupled substitution of Li^{+} and $HREE^{3+}$ with 2 Mg,Fe^{2+}. Garnet rims that grew during peak-metasomatic conditions are relatively Li-poor due to co-crystallization of omphacite, which strongly prefers Li relative to garnet (Marschall et al., 2007a). Comparing the different zoisite eclogite samples, Li contents in omphacite are relatively homogenous, suggesting a more penetrative metasomatism than in the MORB-type eclogites and/or re-equilibration in omphacite aided by the presence of the metasomatic fluid.

Oxygen isotope compositions of garnet from the zoisite eclogites show a smaller range than the MORB-type eclogites, but still with observable differences between samples (Fig. 5). This suggests a metasomatic overprint that did not entirely lead to full equilibration (Baker et al., 1997). O isotopic fractionation between individual mineral pairs including garnet is mostly out of equilibrium. For instance, $\Delta^{18}O_{omph\text{-}grt}$ is always negative (-0.7 to -2.3 ‰), whereas positive fractionations are to be expected at eclogite-facies equilibrium conditions. Disequilibria between zoisite and garnet for two of the three analyzed zoisite eclogite samples (SEC 31-2-2 and 31-2-3 with $\Delta^{18}O_{zoisite\text{-}grt}$ = -0.8 and -1.8 ‰, respectively) are also evident compared to the theoretical values for equilibrium O isotope fractionation at 500-800 °C ($\Delta^{18}O_{zoisite\text{-}grt}$ = +1.6 to +0.9 ‰; calculated based on Zheng, 1993a, 1993b) and point to an external fluid source and partial equilibration only, related to different reactivities among the affected minerals. Zoisite-omphacite pairs of the Raspas zoisite eclogites, however, are close to equilibrium for two samples, suggesting that both these minerals have equilibrated with the metasomatic fluid more fully than garnet. In summary, the O isotope fractionation in the zoisite eclogites shows variable deviations from equilibrium, which has to be explained. Since there are no relics of a magmatic texture in the zoisite eclogites, inheritance from precursor minerals is an unlikely reason for the disequilibria. Accessory mineral inclusions in garnet and omphacite are not more abundant than in the MORB-type eclogites, so they are probably also not the major cause for disequilibria. One possible explanation, advocated by Zheng et al. (1993b), states that omphacite recrystallized by incorporating structural OH, which is significantly depleted in ^{18}O relative to anhydrous silicates. On the other hand, garnet is considered as most resistant to O isotopic changes via fluid infiltration due to its low solubility (Gregory and Criss, 1986), and hence, garnet cores may not have reached isotopic

equilibrium with the metasomatic fluid. They would then retain an O isotopic signature out of equilibrium with omphacite and zoisite that completely recrystallized during the metasomatic event by dissolution-precipitation mechanisms. The observed shift in $\delta^{18}O$ in omphacite is in agreement with a greater solubility of omphacite compared to garnet and with variable degrees of partial exchange with a high-$\delta^{18}O$ fluid, as observed for olivine-clinopyroxene pairs in peridotite xenoliths (Gregory and Taylor, 1986). This would imply that garnet rims have a lighter O isotopic signature than garnet cores. Such a feature has been observed in regional metamorphic garnets from Vermont and accordingly, the O isotope zoning pattern was interpreted as a result of fluid infiltration during later stages of garnet growth (Chamberlain and Conrad, 1991).

The homogeneous Sr-Nd isotopic compositions of the zoisite eclogites are similar to the one of the zoisite vein and suggest that this signature is completely inherited from the vein-forming metasomatic fluid (Fig. 6). This similarity in the Sr-Nd isotope signature is also a strong argument against inheritance from the zoisite eclogites' precursor rock. Instead, the metasomatic formation of zoisite in the eclogites by the vein-forming fluids is the cause for the Sr-Nd isotope homogenization, because zoisite is the main carrier of both Sr (up to ~8000 ppm) and Nd (up to ~600 ppm) (Herms et al., submitted). However, the small spread in $^{147}Sm/^{144}Nd$ ratios (0.115-0.121) and the very low concentrations of radiogenic ^{87}Rb coupled to an extremely small spread in $^{87}Rb/^{86}Sr$ ratios (0.008-0.016) does not permit to define a reasonable isochron. A fluid-dominated Sr isotope signal was also observed in HP mélange rocks from the Catalina Schist (California), although Nd isotopes behaved more conservatively in this case (King et al., 2006).

Like the MORB-type eclogites, the zoisite eclogites are enriched in Li and characterized by negative $\delta^{7}Li$ values. The most straightforward explanation is a fluid-induced Li enrichment coupled with kinetic Li isotope fractionation, as for the MORB-type eclogites and other orogenic eclogites worldwide (Marschall et al., 2007b). In the blueschists, more homogeneous and mostly positive $\delta^{7}Li$ values point to less intense metasomatic effects. In summary, Sr-Nd-O-Li isotope systematics of the zoisite eclogites provide clear evidence for pervasive metasomatism along vein-like flow structures involving a channelized external fluid. A major difference to the limited chemical changes in the MORB-type eclogites is that the zoisite eclogites were affected by larger fluid fluxes that interacted more intensely with a higher proportion of minerals. The system was fluid-dominated and consequently, the zoisite eclogites were significantly affected by the chemical load of the fluid.

5.4. Constraints on fluid sources

Three potential fluid source rocks are to be considered to be of importance in generating the metasomatic subduction zone fluids responsible for the chemical and isotopic changes observed in the Raspas eclogites: Subducted basaltic oceanic crust, the overlying subducted sediments and deserpentinizing mantle rock, which may include both subducted abyssal peridotites and fore-arc mantle wedge.

In the MORB-type eclogites, the constant, MORB-like εNd values and the preservation of a seafloor alteration trend in the Sr isotopes suggest that input from sedimentary sources, which have much less radiogenic Nd isotope signatures than MORB, could not have been significant (Fig. 6). High-pressure serpentinites, associated dehydration veins and fluids derived from serpentinites have low Li contents (Scambelluri et al., 2004), which makes them an unlikely source for the metasomatism observed in the MORB-type eclogites. The isotopic evidence for localized fluid flow and the Li enrichment is most consistent with a MORB dehydration fluid affecting the MORB-type eclogites. Lithium enrichment in the MORB-type eclogites clearly points towards a Li-rich fluid, and MORB-dehydration fluids constitute a potential Li source because they can be significantly enriched in Li (up to 200 ppm) due to rock-fluid partition coefficients of 0.06-0.13 (Marschall et al., 2007a). To maintain the high Li contents from the MORB-fluid in the rock, the fluid needs to be at least partly consumed during recrystallization in the eclogite facies. The presence of texturally equilibrated amphibole as hydrous phase points to the presence of a hydrous fluid during eclogite recrystallization. Lithium is then preferentially incorporated into co-crystallizing omphacite because it is more compatible in omphacite compared to Ca-rich amphibole ($D^{Li}_{Ca\text{-}amphibole/omphacite}$ = 0.04; Marschall et al., 2007a). Although the Li isotopic signature of MORB dehydration fluids is likely to be positive and elevated, this signal will be erased by diffusive isotope fractionation of Li isotopes during fluid-rock interaction. A negative correlation of δ^7Li with δ^{15}N (Fig. 7d) for MORB-type eclogites and blueschists suggests that the metasomatic event produced correlated changes in both parameters. However, more data are required to evaluate whether these trends indicate a correlated magnitude of metasomatic alteration or whether N isotopes may also be significantly fractionated by diffusion.

A detailed fluid inclusion study by Herms et al. (submitted) in the zoisite eclogites indicates large-scale fluid flow and an external fluid supply based on the constant fluid composition and the presence of these fluid inclusions in different minerals of the zoisite

eclogites. The pervasive metasomatism in the zoisite eclogites, leading to ubiquitous crystallization of zoisite and Sr-Nd isotope homogenization, is also suggestive of a large fluid flux, in agreement with the fluid inclusion data. In fact, a large fluid flux can be attributed to dehydration of serpentinites, which constitute the most important fluid reservoir of subducting slabs (e.g., Ulmer and Trommsdorff, 1995). However, the high $\delta^{18}O$ and low εNd values combined with elevated Li contents provide evidence for a (meta)sedimentary contribution to these fluids.

Global subducted sediment has Li concentrations of 2-75 ppm (Bouman et al., 2004) and a mass-weighted mean of 43.3 ppm Li (Chan et al., 2006), and sediment-derived fluids would be even more enriched if a mineral-fluid partition coefficient of 0.2 (Brenan et al., 1998) were taken into account. Subducted metasediments may contain >10 modal % of chlorite (Li et al., 2008), which can incorporate significant amounts of Li (up to 100 ppm; Bebout et al., 2007). Chlorite breakdown to garnet and H_2O releases 1.4 wt.% of H_2O at depths of 50-60 km, hence these sediment-derived fluids will be Li-rich. This depth range is close to the peak P-T conditions of the Raspas eclogites, suggesting that fluids derived from chlorite breakdown in metasediments may have been a component of the metasomatizing agent.

The O isotope composition of an aqueous fluid in equilibrium with vein zoisite can be calculated based on zoisite-water fractionation factors given by Zheng (1993b). At temperatures of 500-600°C, the fluid composition would be in the range +13 to +13.5‰. These elevated $\delta^{18}O$ values in the fluid are best reconciled with a fluid derived from the dehydration of oceanic sediments ($\delta^{18}O$ = +11.5 to +28.5‰; Savin and Epstein, 1970). Most importantly, the negative εNd values make a fluid component derived from subducted sediments most plausible. Although altered oceanic peridotites (Snow and Reisberg, 1995) have Sr-Nd isotope signatures similar to the zoisite eclogites, a sole contribution of an altered peridotite source to the Raspas zoisite eclogites is unlikely because of two reasons: First, harzburgite and serpentinite from the Raspas complex, which constitute a potential fluid source, do not show the required Sr-Nd isotope characteristics (Bosch et al., 2002). Second, extremely low Nd contents (< 1 ppm) and generally low Sr contents (< 10 ppm) in the altered peridotites would require a contributions of > 99% from this source to reach the zoisite eclogite composition if bulk mixing is assumed and > 90% if a 20fold enrichment of Sr and Nd is taken into account for a hypothetical fluid derived from the altered peridotites. Such a large external input to generate the zoisite eclogites is highly unlikely because they still have overall basaltic major element chemistry.

Mixing of sedimentary components to a MORB-like eclogitic component is illustrated by several mixing lines in Fig. 6. As bulk mixing is unlikely, the curves simply illustrate the consequences of contamination of the eclogite with (meta)sedimentary contaminants with moderately high $^{87}Sr/^{86}Sr$ ratios and highly negative εNd values. The actual contamination process will be complex, as it involves fluid for which compositions are more difficult to constrain as well as mineral phases that have different dissolution and precipitation rates while reacting with the fluid (e.g., Putnis and John, 2010). Given the large natural variations in Sr-Nd isotope compositions and in Sr and Nd concentrations of subducting sediments and the fact that solid-fluid partition coefficient for sediment for Sr and Nd are close to 1 at appropriate temperatures of 650° and 700°C (Johnson and Plank, 1999), bulk mixing can be used as a simplifying model for comparative purposes. Admixing of a metasedimentary component as sampled in the Raspas complex (Bosch et al., 2002; this study) to a MORB-type eclogite produces mixing trajectories that come close to the composition of the zoisite vein and the zoisite eclogites. Terrigenous sediments, represented by sediments from the Lesser Antilles arc, possess the appropriate Sr-Nd isotope characteristics to produce zoisite eclogite compositions in Sr-Nd isotope space by mixing. This suggests that a fluid component derived from terrigenous sediments was involved in the genesis of the zoisite eclogites. A contribution from metasediments is also indicated by the elevated LREE and LILE contents in the zoisite eclogites (Spandler et al., 2003, 2004), even though some of these fluid-mobile elements can also be enriched in serpentinites (Paulick et al., 2006; Scambelluri et al., 2001) and may be mobilized during channelized fluid flow in subducted oceanic crust (Zack and John, 2007).

Having established that a (meta)sedimentary fluid component was added to the fluid flux through the slab, which probably is largely derived from serpentinite dehydration, we will now evaluate how these fluids were mixed and how they metasomatized the eclogitized basaltic crust. A first possibility is that the fluid is derived from sediments that were more deeply subducted than the eclogites, causing fluid flow along the slab-wedge interface that could enter the eclogites at a somewhat higher structural level, mixing along their way with serpentine-derived fluid. A second option is that sediments were intercalated with the oceanic crust, and trace elements from these sediments were either leached from a passing serpentinite-derived fluid or mobilized by dehydration reactions, such as breakdown of chlorite. A distinction of these models based on geochemical data is not possible, but both scenarios are conceivable for the Raspas Complex.

6. Conclusions

1. In the Raspas Complex (Ecuador), two distinct types of eclogites can be identified based on petrography and geochemistry: MORB-type eclogites with geochemical similarities to MORB and zoisite eclogites that are enriched in LREE and other trace elements. The two eclogite types show different evidence for distinct metasomatic processes.
2. MORB-type eclogites show evidence for seafloor alteration based on O and Sr isotopes. A small-scale, non-pervasive metasomatic overprint in the MORB-type eclogites is indicated by elevated Li contents and highly negative δ^7Li values, the latter caused by kinetic isotope fractionation.
3. Zoisite eclogites show evidence for significant pervasive fluid overprint based on relatively homogenous O, Sr and Nd isotopic compositions. Sr and Nd isotope signatures of the zoisite eclogites are similar to an associated zoisite vein, providing evidence for a fluid-derived signal.
4. Different magnitudes of fluid flux result in rock-dominated (MORB-type eclogites) and fluid-dominated (zoisite eclogites) systems. In the rock-dominated system, the fluid was most likely of local origin and caused little fluid-mineral interactions with only minor chemical changes of the eclogite. In dehydrating metabasalts that transform from blueschist into eclogite, small amounts of fluid predominately move along grain boundaries, so that chemical and isotopic compositions of the minerals are largely preserved. In contrast, the fluid-dominated system has been much more reactive and the external fluids significantly changed the precursor composition of the zoisite eclogites. Reactive minerals, such as omphacite and zoisite, were in particular affected, whereas garnet was the least reactive mineral.
5. The source of the metasomatic fluid affecting the MORB-type eclogites is probably derived from dehydration of oceanic crust with only localized occurrence. In contrast, the fluid that caused pervasive metasomatism in the zoisite eclogites is considered a mixture of serpentinite dehydration fluid with a sedimentary component.
6. Chemical processing of subducted rocks by metasomatic fluids can significantly alter the precursor geochemistry and should be considered in any attempt to trace or mass-balance recycling at convergent margins.

Acknowledgments

We thank A. Pack and R. Przybilla for oxygen isotope analyses, C. Kusebauch for handpicking of mineral separates and H. Brätz for help with laser ICP-MS analyses. R.L. Rudnick and W.F. McDonough generously provided access to Li isotope analyses, supported by NSF grant EAR0609689. We are grateful to T. Toulkeridis and P. Cabrera for guidance and company in the field area. Constructive reviews by S. Penniston-Dorland and F.-Z. Teng helped to improve the manuscript, and B. Bourdon is thanked for editorial handling. This is contribution no. 189 of the Sonderforschungsbereich (SFB) 574 “Volatiles and Fluids in Subduction Zones” at Kiel University.

References

Arculus, R.J., Lapierre, H., Jaillard, E., 1999. Geochemical window into subduction and accretion processes: Raspas metamorphic complex, Ecuador. Geology 27, 547-550.

Austrheim, H., 1987. Eclogitization of lower crustal granulites by fluid migration through shear zones. Earth Planet. Sci. Lett. 81, 221-232.

Baker, J., Matthews, A., Mattey, D., Rowley, D., Xue, F., 1997. Fluid-rock interactions during ultra-high pressure metamorphism, Dabie Shan, China. Geochim. Cosmochim. Acta 61, 1685-1696.

Barnicoat, A.C., Cartwright, I., 1995. Focused fluid flow during subduction: Oxygen isotope data from high-pressure ophiolites of the western Alps. Earth Planet. Sci. Lett. 132, 53-61.

Bebout, G.E., 1991. Field-based evidence for devolatilization in subduction zones: Implications for arc magmatism. Science 251, 413-416.

Bebout, G.E., 2007. Metamorphic chemical geodynamics of subduction zones. Earth Planet. Sci. Lett. 260, 373-393.

Bebout, G.E., Bebout, A.E., Graham, C., 2007. Cycling of B, Li, and LILE (K, Cs, Rb, Ba, Sr) into subduction zones: SIMS evidence from micas in high-P/T metasedimentary rocks. Chem. Geol. 239, 284-304.

Bebout, G.E., Barton, M.D., 1993. Metasomatism during subduction: products and possible paths in the Catalina Schist, California. Chem. Geol. 180, 61-92.

Beinlich, A., Klemd, R., John, T., Gao, J., 2010. Trace-element mobilization during Ca-metasomatism along a major fluid conduit: Eclogitization of blueschist as a consequence of fluid-rock interaction. Geochim. Cosmochim. Acta 74, 1892-1922.

Berger, J., Féménias, O., Ohnenstetter, D., Bruguier, O., Plissart, G., Mercier, J.-C.C., Demaiffe, D., 2010. New occurrence of UHP eclogites in Limousin (French Massif Central): Age, tectonic setting and fluid-rock interactions. Lithos 118, 365-382.

Bosch, D., Gabriele, P., Lapierre, H., Malfere, J.-L., Jaillard, E., 2002. Geodynamic significance of the Raspas Metamorphic Complex (SW Ecuador): geochemical and isotopic constraints. Tectonophysics 345, 83-102.

Bouman, C., Elliott, T., Vroon, P.Z., 2004. Lithium inputs to subduction zones. Chem. Geol. 212, 59-79.

Boynton, W.V., 1984. Geochemistry of the rare earth elements: meteorite studies, in Henderson, P. (Ed.), Rare Earth Element Geochemistry. Elsevier, Amsterdam, pp. 63-114.

Breeding, C.M., Ague, J.J., Bröcker, M., 2004. Fluid-metasedimentary rock interactions in subduction-zone mélange: Implications for the chemical composition of arc magmas. Geology 32, 1041-1044.

Brenan, J.M., Ryerson, F.J., Shaw, H.F., 1998. The role of aqueous fluids in the slab-to-mantle transfer of boron, beryllium, and lithium during subduction: Experiments and models. Geochim. Cosmochim. Acta 62, 3337-3347.

Burke, W.H., Denison, R.E., Hetherington, E.A., Koepnick, R.B., Nelson, H.F., Otto, J.B., 1982. Variations of seawater $^{87}Sr/^{86}Sr$ throughout Phanerozoic time. Geology 10, 516-519.

Chamberlain, C.P., Conrad, M.E., 1991. Oxygen isotope zoning in garnet. Science 254, 403-406.

Chan, L.-H., Alt, J.C., Teagle, D.A.H., 2002. Lithium and lithium isotope profiles through the upper oceanic crust: a study of seawater-basalt exchange at ODP Sites 504B and 896A. Earth Planet. Sci. Lett. 201, 187-201.

Chan, L.-H., Edmond, J.M., Thompson, G., Gillis, K., 1992. Lithium isotopic composition of submarine basalts: Implications for lithium cycle in the oceans. Earth Planet. Sci. Lett. 108, 151-160.

Chan, L.-H., Leeman, W.P., Plank, T., 2006. Lithium isotopic composition of marine sediments. Geochem. Geophys. Geosys. 7(6), Q06005, doi:10.1029/2005GC001202.

Cocker, J.D., Griffin, B.J., Muehlenbachs, K., 1982. Oxygen and carbon isotope evidence for seawater-hydrothermal alteration of the Macquarie Island ophiolite. Earth Planet. Sci. Lett. 61, 112-122.

DePaolo, D.J., 1988. Neodymium isotope geochemistry: An introduction. Springer, New York.

Eiler, J.M., Schiano, P., Kitchen, N., Stolper, E.M., 2000. Oxygen-isotope evidence for recycled crust in the sources of mid-ocean-ridge basalts. Nature 403, 530-534.

Feininger, T., 1978. Mapa geológico de la parte occidental de la Provincia de El Oro [1:50,000]. Quito. Inst. Geog. Militar.

Feininger, T., 1980. Eclogite and related high-pressure regional metamorphic rocks from the Andes of Ecuador. J. Petrol. 21, 107-140.

Gabriele, P., 2002. HP terranes exhumation in an active margin setting: geology, petrology and geochemistry of the Raspas Complex in SW Ecuador. Unpublished Ph.D. thesis, University of Lausanne, Switzerland.

Gabriele, P., Ballèvre, M., Jaillard, E., Hernandez, J., 2003. Garnet-chloritoid-kyanite metapelites from the Raspas Complex (SW Ecuador): a key eclogite-facies assemblage. Eur. J. Mineral. 15, 977-989.

Gao, J., John, T., Klemd, R., Xiong, X., 2007. Mobilization of Ti-Nb-Ta during subduction: Evidence from rutile-bearing dehydration segregations and veins hosted in eclogite, Tianshan, NW China. Geochim. Cosmochim. Acta 71, 4974-4996.

Gerya, T.V., Stöckhert, B., Perchuk, A.L., 2002. Exhumation of high-pressure metamorphic rocks in a subduction channel: A numerical simulation. Tectonics 21(6), 1056, doi:10.1029/2002TC001406.

Gieré, R., Williams, C.T., 1992. REE-bearing minerals in a Ti-rich vein from the Adamello contact aureole (Italy). Contrib. Mineral. Petrol. 112, 83-100.

Glodny, J., Austrheim, H., Molina, J.F., Rusin, A., Seward, D., 2003. Rb/Sr record of fluid-rock interaction in eclogites: The Marun-Keu complex, Polar Urals, Russia. Geochim. Cosmochim. Acta 67, 4353-4371.

Glodny, J., Kühn, A., Austrheim, H., 2008. Diffusion versus recrystallization processes in Rb-Sr geochronology: Isotopic relics in eclogite facies rocks, Western Gneiss Region, Norway. Geochim. Cosmochim. Acta 72, 506-525.

Goldstein, S.L., O'Nions, R.K., Hamilton, P.J., 1984. A Sm-Nd study of atmospheric dusts and particulates from major river systems. Earth Planet. Sci. Lett. 70, 221-236.

Gregory, R.T., Criss, R.E., 1986. Isotopic exchange in open and closed systems, in Valley, H.P., Taylor, H.P., O'Neil, J.R. (Eds.), Stable isotopes in high temperature geological processes. Mineralogical Society of America, Reviews in Mineralogy and Geochemistry vol. 16, pp. 91-127.

Gregory, R.T., Taylor, H.P., 1981. An oxygen isotope profile in a section of Cretaceous oceanic crust, Samail ophiolite, Oman: Evidence for $\delta^{18}O$ buffering of the oceans by deep (> 5 km) seawater-hydrothermal circulation at mid-ocean ridges. J. Geophys. Res. 86 (B4), 2737-2755.

Gregory, R.T., Taylor, H.P., 1986. Non-equilibrium, metasomatic $^{18}O/^{16}O$ effects in upper mantle mineral assemblages. Contrib. Mineral. Petrol. 93, 124-135.

Halama, R., Bebout, G.E., John, T., Schenk, V., 2010. Nitrogen recycling in subducted oceanic lithosphere: The record in high- and ultrahigh-pressure metabasaltic rocks. Geochim. Cosmochim. Acta 74, 1636-1652.

Halama, R., McDonough, W.F., Rudnick, R.L., Bell, K., 2008. Tracking the lithium isotopic evolution of the mantle using carbonatites. Earth Planet. Sci. Lett. 265, 726-742.

Halama, R., McDonough W.F., Rudnick, R.L., Keller, J., Klaudius, J., 2007. The Li isotopic composition of Oldoinyo Lengai: Nature of the mantle sources and lack of isotopic fractionation during carbonatite petrogenesis. Earth Planet. Sci. Lett. 254, 77-89.

Halama, R., Savov, I.P., Rudnick, R.L., McDonough, W.F., 2009. Insights into Li and Li isotope cycling and sub-arc metasomatism from veined mantle xenoliths, Kamchatka. Contrib. Mineral. Petrol. 158, 197-222.

Hanrahan, M., Brey, G., Woodland, A., Seitz, H.-M., Ludwig, T., 2009. Li as barometer for bimineralic eclogites: Experiments in natural systems. Lithos, 112S: 992-1001.

Hauff, F., Hoernle, K., Schmidt, A., 2003. Sr-Nd-Pb composition of Mesozoic Pacific oceanic crust (Site 1149 and 801, ODP Leg 185): Implications for alteration of ocean crust and the input into the Izu-Bonin-Mariana subduction system. Geochem. Geophys. Geosys. 4 (8), 8913, doi:10.1029/2002GC000421.

Herms, P., John, T., Bakker, R.J., Schenk, V., submitted. Evidence for channelized external fluid flow and element transfer in subducting slabs (Raspas Complex, Ecuador). Chem. Geol.

Hoernle, K.A., Tilton, G.R., 1991. Sr-Nd-Pb isotope data for Fuerteventura (Canary Islands) basal complex and subaerial volcanics: applications to magma genesis and evolution. Schweiz. Mineral. Petrogr. Mitt. 71, 3-18.

Horodyskyj, U., Lee, C.-T.A., Luffi, P., 2009. Geochemical evidence for exhumation of eclogite via serpentinite channels in ocean-continent subduction zones. Geosphere 5, 426-438.

John, T., Klemd, R., Gao, J., Garbe-Schönberg, C.-D., 2008. Trace-element mobilization in slabs due to non steady-state fluid-rock interaction: Constraints from an eclogite-facies transport vein in blueschist (Tianshan, China). Lithos 103, 1-24.

John, T., Scherer, E.E., Haase, K., Schenk, V., 2004. Trace element fractionation during fluid-induced eclogitization in a subducting slab: trace element and Lu-Hf-Sm-Nd isotope systematics. Earth Planet. Sci. Lett. 227, 441-456.

John, T., Scherer, E., Schenk, V., Herms, P., Halama, R., Garbe-Schönberg, D., 2010. Subducted seamounts in an eclogite-facies ophiolite sequence: The Andean Raspas Complex, SW Ecuador. Contrib. Mineral. Petrol. 159, 265-284.

Johnson, M.C., Plank, T., 1999. Dehydration and melting experiments constrain the fate of subducted sediments. Geochem. Geophys. Geosys. 1, 12, doi:10.1029/1999GC000014

Kelley, K.A., Plank, T., Ludden, J., Staudigel, H., 2003. Composition of altered oceanic crust at ODP sites 801 and 1149. Geochem. Geophys. Geosys. 4, 8910, doi:10.1029/2002GC000435.

King, R.L., Bebout, G.E., Kobayashi, K., Nakamura, E., van der Klauw, S.N.G.C., 2004. Ultrahigh-pressure metabasaltic garnets as probes into deep subduction zone chemical cycling. Geochem. Geophys. Geosys. 5, Q12J14, doi:10.1029/2004GC000746.

King, R.L., Bebout, G.E., Moriguti, T., Nakamura, E., 2006. Elemental mixing systematics and Sr-Nd isotope geochemistry of mélange formation: Obstacles to identification of fluid sources to arc volcanics. Earth Planet. Sci. Lett. 246, 288-304.

Li, Y., Massonne, H.-J., Willner, A., Tang, H.-F., Liu, C.-Q., 2008. Dehydration of clastic sediments in subduction zones: Theoretical study using thermodynamic data of minerals. Island Arc 17, 577-590.

Liebscher, A., Franz, G., Frei, D., Dulski, P., 2007. High-pressure melting of eclogite and the P-T-X history of tonalitic to trondhjemitic zoisite-pegmatites, Münchberg Massif, Germany. J. Petrol. 48, 1001-1019.

Manning, C., 2004. The chemistry of subduction-zone fluids. Earth Planet. Sci. Lett. 223, 1-16.

Marschall, H.R., Altherr, R., Gméling, K., Kasztovszky, Z., 2009. Lithium, boron and chlorine as tracers for metasomatism in high-pressure metamorphic rocks: a case study from Syros (Greece). Mineral. Petrol. 95, 291-302.

Marschall, H.R., Altherr, R., Ludwig, T., Kalt, A., Gméling, K., Kasztovszky, Z., 2006. Partitioning and budget of Li, Be and B in high-pressure metamorphic rocks. Geochim. Cosmochim. Acta 70, 4750-4769.

Marschall, H.R., Altherr, R., Rüpke, L., 2007a. Squeezing out the slab - modelling the release of Li, Be and B during progressive high-pressure metamorphism. Chem. Geol. 239, 323-335.

Marschall, H.R., Pogge von Strandmann, P.A.E., Seitz, H.-M., Elliott, T., Niu, Y., 2007b. The lithium isotopic composition of orogenic eclogites and deep subducted slabs. Earth Planet. Sci. Lett. 262, 563-580.

Meagher, E.P., 1982. Silicate garnets, in Ribbe, P.H. (Ed.), Orthosilicates. Mineralogical Society of America, Chelsea, Michigan, Reviews in Mineralogy vol. 5, pp. 25-66.

McCulloch, M.T., Gregory, R.T., Wasserburg, G.J., Taylor, H.P., 1981. Sm-Nd, Rb-Sr, and 18O/16O isotopic systematics in an oceanic crustal section: Evidence from the Samail ophiolite. J. Geophys. Res. 86 (B4), 2721-2735.

Miller, C., Stosch, H.-G., Hoernes, S., 1988. Geochemistry and origin of eclogites from the type locality Koralpe and Saualpe, Eastern Alps, Austria. Chem. Geol. 67, 103-118.

Molina, J.F., Poli, S., Austrheim, H., Glodny, J., Rusin, A., 2004. Eclogite-facies vein systems in the Marun-Keu complex (Polar Urals, Russia): textural, chemical and thermal constraints for patterns of fluid flow in the lower crust. Contrib. Mineral. Petrol. 147, 487-504.

Nelson, B.K., 1995. Fluid flow in subduction zones: evidence form Nd- and Sr-isotope variations in metabasalts of the Franciscan complex, California. Contrib. Mineral. Petrol. 119, 247-262.

Niu, Y., Batiza, R., 1997. Trace element evidence from seamounts for recycled oceanic crust in the eastern Pacific mantle. Earth Planet. Sci. Lett. 148, 471-483.

Pack, A., Toulouse, C., Przybilla, R., 2007. Determination of oxygen triple isotope ratios without cryogenic separation of NF3 - technique with application to analyses of technical O_2 gas and meteorite classification. Rapid Commun. Mass Spectrom. 21, 3721-3728.

Paquin, J., Altherr, R., Ludwig, T., 2004. Li-Be-B systematics in the ultrahigh-pressure garnet peridotite from Alpe Arami (Central Swiss Alps): implications for slab-to-mantle wedge transfer. Earth Planet. Sci. Lett. 218, 507-519.

Paulick, H., Bach, W., Godard, M., De Hoog, J.C.M., Suhr, G., Harvey, J., 2006. Geochemistry of abyssal peridotites (Mid-Atlantic Ridge, 15°20'N, ODP Leg 209): Implications for fluid/rock interaction in slow spreading environments. Chem. Geol. 234, 179-210.

Pearce, N.J.G., Perkins, W.T., Westgate, J.A., Gorton, M.P., Jackson, E.E., Neal, C.R., Chenery, S.P., 1997. A compilation of new and published major and trace element data for NIST SRM 610 and NIST SRM 612 glass reference materials. Geostandard Newsletters 21, 115-144.

Penniston-Dorland, S.C., Sorensen, S.S., Ash, R.D., Khadke, S.V., 2010. Lithium isotopes as tracer of fluids in a subduction zone mélange: Franciscan Complex, CA. Earth Planet. Sci. Lett. 292, 181-190.

Peucat, J.J., Vidal, P., Bernard-Griffiths, J., Condie, K.C., 1988. Sr, Nd and Pb isotopic systems in the Archean low- to high-grade transition zone of southern India: syn-accretion vs. post-accretion granulites. J. Geol. 97, 537-550.

Philippot, P., Busigny, V., Scambelluri, M., Cartigny, P., 2007. Oxygen and nitrogen isotopes as tracers of fluid activities in serpentinites and metasediments during subduction. Mineral. Petrol. 91, 11-24.

Plank, T., Langmuir, C.H., 1998. The chemical composition of subducting sediment and its consequences for the crust and mantle. Chem. Geol. 145, 325-394.

Putlitz, B., Matthews, A., Valley, J.W., 2000. Oxygen and hydrogen isotope study of high-pressure metagabbros and metabasalts (Cyclades, Greece): implications for the subduction of oceanic crust. Contrib. Mineral. Petrol. 138, 114-126.

Putnis, A., John, T., 2010. Replacement processes in the Earth's crust. Elements 6, 159-164.

Qi, H.P., Taylor, P.D.P., Berglund, M., De Bievre, P., 1997. Calibrated measurements of the isotopic composition and atomic weight of the natural Li isotopic reference material IRMM-016. Int. J. Mass Spectrom. Ion Process. 171, 263-268.

Richter, F.M., Davis, A.M., DePaolo, D.J., Watson, E.B., 2003. Isotope fractionation by chemical diffusion between molten basalt and Rhyolite. Geochim. Cosmochim. Acta 67, 3905-3923.

Rudnick, R.L., Tomascak, P.B., Heather, B.N., Gardner, L.R., 2004. Extreme lithium isotopic fractionation during continental weathering revealed in saprolites from South Carolina. Chem. Geol. 212, 45-57.

Ryan, J.G., Langmuir, C.H., 1987. The systematics of lithium abundances in young volcanic rocks. Geochim. Cosmochim. Acta 51, 1727-1741.

Savin, S.M., Epstein, S., 1970. The oxygen and hydrogen isotope geochemistry of ocean sediments and shales. Geochim. Cosmochim. Acta 34, 43-63.

Scambelluri, M., Bottazzi, P., Trommsdorff, V., Vannucci, R., Hermann, J., Gòmez-Pugnaire, M.T., Lòpez-Sànchez Vizcaìno, V., 2001. Incompatible element-rich fluids released by antigorite breakdown in deeply subducted mantle. Earth Planet. Sci. Lett. 192, 457-470.

Scambelluri, M., Fiebig, J., Malaspina, N., Müntener, O., Pettke, T., 2004. Serpentinite subduction: implications for fluid processes and trace-element recycling. Int. Geol. Rev. 46, 593-613.

Scambelluri, M., Hermann, J., Morten, L., Rampone, E., 2006. Melt- versus fluid-induced metasomatism in spinel to garnet wedge peridotites (Ulten Zone, Eastern Italian Alps): clues from trace element and Li abundances. Contrib. Mineral. Petrol. 151, 372-394.

Schmidt, M.W., Poli, S., 1998. Experimentally based water budgets for dehydrating slabs and consequences for arc magma generation. Earth Planet. Sci. Lett. 163, 361-379.

Schulz, B., Klemd, R., Brätz, H., 2006. Host rock compositional controls on zircon trace element signatures in metabasites from the Austroalpine basement. Geochim. Cosmochim. Acta 70, 697-710.

Sharp, Z.D., 1990. A laser-based microanalytical method for the in situ determination of oxygen isotope ratios of silicates and oxides. Geochim. Cosmochim. Acta 54, 1353-1357.

Simons, K.K. et al., 2010. Lithium isotopes in Guatemalan and Franciscan HP-LT rocks: Insights into the role of sediment-derived fluids during subduction. Geochim. Cosmochim. Acta, 74, 3621-3641.

Snow, J.E., Reisberg, L., 1995. Os isotopic systematics of the MORB mantle: results from altered abyssal peridotites. Earth Planet. Sci. Lett. 133, 411-421.

Sorensen, S.S., Grossman J.N., 1989. Enrichment of trace elements in garnet amphibolites from a paleo-subduction zone: Catalina Schist, southern California. Geochim. Cosmochim. Acta 53, 3155-3177.

Sorensen, S.S., Grossman, J.N., Perfit, M.R., 1997. Phengite-hosted LILE-enrichment in eclogite and related rocks: implications for fluid-mediated mass-transfer in subduction zones and arc magma genesis. J Petrol. 38, 3-34.

Spandler, C., Hermann, J., 2006. High-pressure veins in eclogite from New Caledonia and their significance for fluid migration in subduction zones. Lithos 89, 135-153.

Spandler, C., Hermann, J., Arculus, R., Mavrogenes, J., 2003. Redistribution of trace elements during prograde metamorphism from lawsonite blueschist to eclogite facies; implications for deep subduction-zone processes. Contrib. Mineral. Petrol. 146, 205-222.

Spandler, C., Hermann, J., Arculus, R., Mavrogenes, J., 2004. Geochemical heterogeneity and element mobility in deeply subducted oceanic crust; insights from high-pressure mafic rocks from New Caledonia. Chem. Geol. 206, 21-42.

Staudigel, H., Muehlenbachs, K., Richardson, S.H., Hart, S.R., 1981. Agents of low temperature ocean crust alteration. Contrib. Mineral. Petrol. 77, 150-157.

Sun, S.-S., McDonough, W.F., 1989. Chemical and isotopic systematics of oceanic basalts: implications for mantle composition and processes, in Saunders, A.D., Norry, M.J. (Eds.), Magmatism in the Ocean Basins. Geological Society, London, Special Publication vol. 42, pp. 313-345.

Taylor, S.R., McLennan, S. M., 1985. The continental crust: its composition and evolution. Blackwell, Oxford.

Teng, F.-Z., McDonough, W.F., Rudnick, R.L., Dalpé, C., Tomascak, P.B., Chappell, B.W., Gao, S., 2004. Lithium isotopic composition and concentration of the upper continental crust. Geochim. Cosmochim. Acta 68, 4167-4178.

Teng, F.-Z., McDonough W.F., Rudnick, R.L., Wing, B.A., 2007. Limited lithium isotopic fractionation during progressive metamorphic dehydration in metapelites: A case study from the Onawa contact aureole, Maine. Chem. Geol. 239, 1-12.

Teng, F.-Z., Rudnick, R.L., McDonough W.F., Gao, S., Tomascak, P.B., Liu, Y., 2008. Lithium isotopic composition and concentration of the deep continental crust. Chem. Geol. 255, 47-59.

Tomascak, P.B., 2004. Developments in the understanding and application of lithium isotopes in the Earth and Planetary Sciences, in Johnson, C.M., Beard, B.L., Albarède, F. (Eds.), Geochemistry of Non-Traditional Stable Isotopes. Mineralogical Society of America, Reviews in Mineralogy and Geochemistry vol. 55, pp. 153-195.

Tomascak, P.B., Langmuir, C.H., le Roux, P.J., Shirey, S.B., 2008. Lithium isotopes in global mid-ocean ridge basalts. Geochim. Cosmochim. Acta 72, 1626-1637.

Ulmer, P., Trommsdorff, V., 1995. Serpentine stability to mantle depths and subduction-related magmatism. Science 268, 858-861.

Valley, J.W., 1986. Stable isotope geochemistry of metamorphic rocks, in Valley, H.P., Taylor, H.P., O'Neil, J.R. (Eds.), Stable isotopes in high temperature geological processes. Mineralogical Society of America, Reviews in Mineralogy and Geochemistry vol. 16, pp. 445-489.

Valley, J.W., Kitchen, N., Kohn, M.J., Niendorf, C.R., Spicuzza, M.J., 1995. UWG-2, a garnet standard for oxygen isotope ratios: Strategies for high precision and accuracy with laser heating. Geochim. Cosmochim. Acta 59, 5223-5231.

Van der Straaten, F., Schenk, V., John, T., Gao, J., 2008. Blueschist-facies rehydration of eclogites (Tian Shan, NW-China): Implications for fluid-rock interaction in the subduction channel. Chem. Geol. 255, 195-219.

Vroon, P.Z., Van Bergen, M.J., Klaver, G.J., White, W.M., 1995. Strontium, neodymium, and lead isotopic and trace-element signatures of the East Indonesian sediments: Provenance and implications for Banda Arc magma genesis. Geochim. Cosmochim. Acta 59, 2573-2598.

Wenger, M., Armbruster, T., 1991. Crystal chemistry of lithium: oxygen coordination and bonding. Eur. J. Mineral. 3, 387-399.

Wunder, B., Meixner, A., Romer, R.L., Heinrich, W., 2006. Temperature-dependent isotopic fractionation on lithium between clinopyroxene and high-pressure hydrous fluids. Contrib. Mineral. Petrol. 151, 112-120.

Zack, T., John, T., 2007. An evaluation of reactive fluid flow and trace element mobility in subducting slabs. Chem. Geol. 239, 199-216.

Zack, T., Tomascak, P.B., Rudnick, R.L., Dalpé, C., McDonough, W.F., 2003. Extremely light Li in orogenic eclogites: The role of isotope fractionation during dehydration in subducted oceanic crust. Earth Planet. Sci. Lett. 208, 279-290.

Zanetti, A., Mazzucchelli, M., Rivalenti, G., Vannucci, R., 1999. The Finero phlogopite-peridotite massif: an example of subduction-related metasomatism. Contrib. Mineral. Petrol. 134, 107-122.

Zheng, Y.-F., 1993a. Calculation of oxygen isotope fractionation in anhydrous silicate minerals. Geochim. Cosmochim. Acta 57, 1079-1091.

Zheng, Y.-F., 1993b. Calculation of oxygen isotope fractionation in hydroxyl-bearing silicates. Earth Planet. Sci. Lett. 120, 247-263.

Zheng, Y.-F., Fu, B., Gong, B., Li, L., 2003. Stable isotope geochemistry of ultrahigh pressure metamorphic rocks from the Dabie-Sulu orogen in China: implications for geodynamics and fluid regime. Earth Sci. Rev. 62, 105-161.

Zheng, Y.-F., Wang, Z.-R., Li, S.-G., Zhao, Z.-F., 2002. Oxygen isotope equilibrium between eclogite minerals and its constraints on mineral Sm-Nd chronometer. Geochim. Cosmochim. Acta 66, 625-634.

Fig. 1. Geological map showing the main lithological units and structures of the El Oro Metamorphic Complex, SW Ecuador (modified after Gabriele (2002) and John et al. (2010)). Eclogite samples were collected along the Rio Raspas. GPS coordinates of analyzed samples are given in Halama et al. (2010) and John et al. (2010).

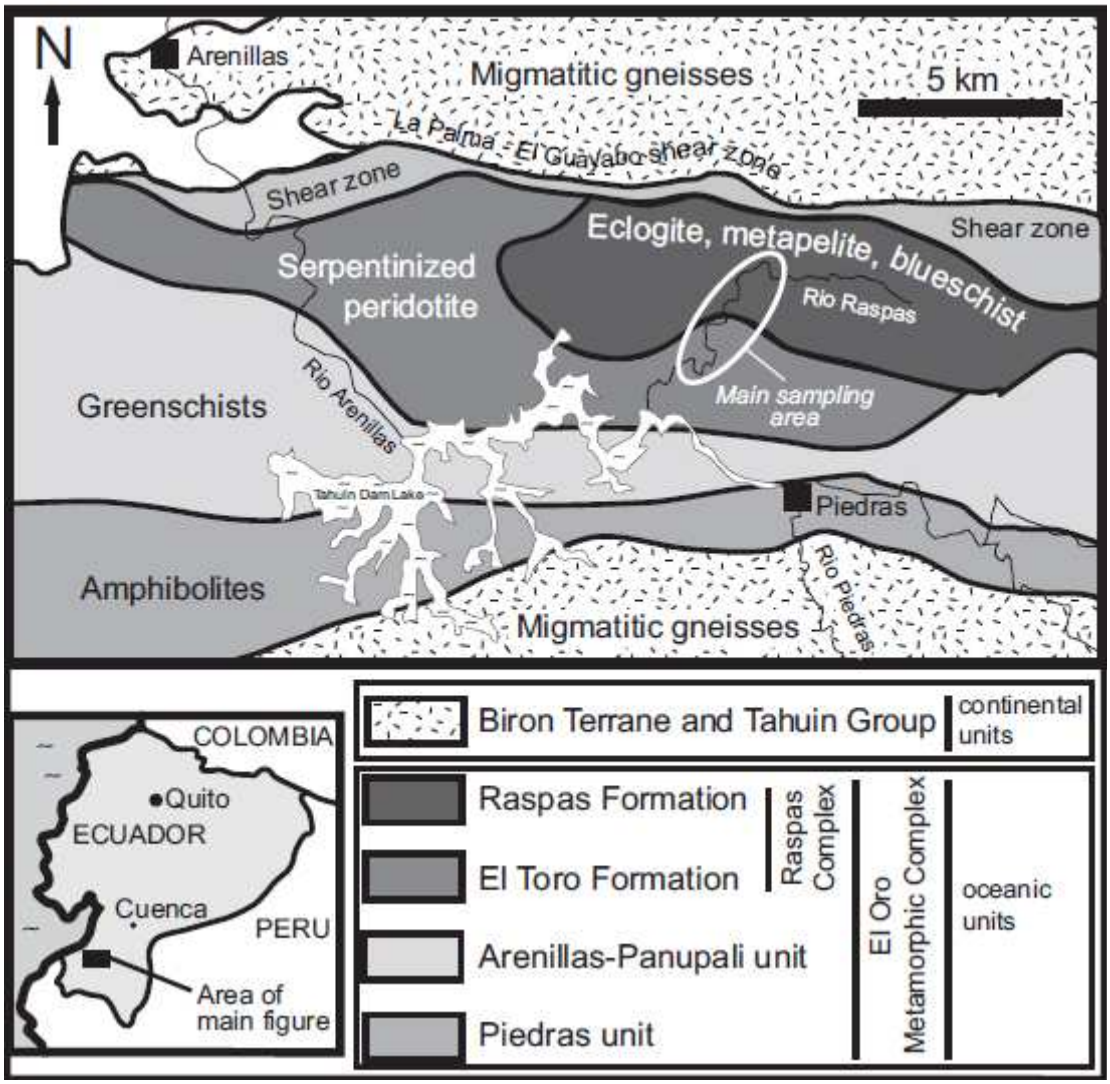

Fig. 2. Chondrite-normalized (Boynton, 1984) REE patterns from Sm to Lu for garnets from a) MORB-type and b) zoisite eclogites of the Raspas Complex (data are from Table 1). Filled and open symbols are core and rim compositions, respectively (C = core, R = rim).

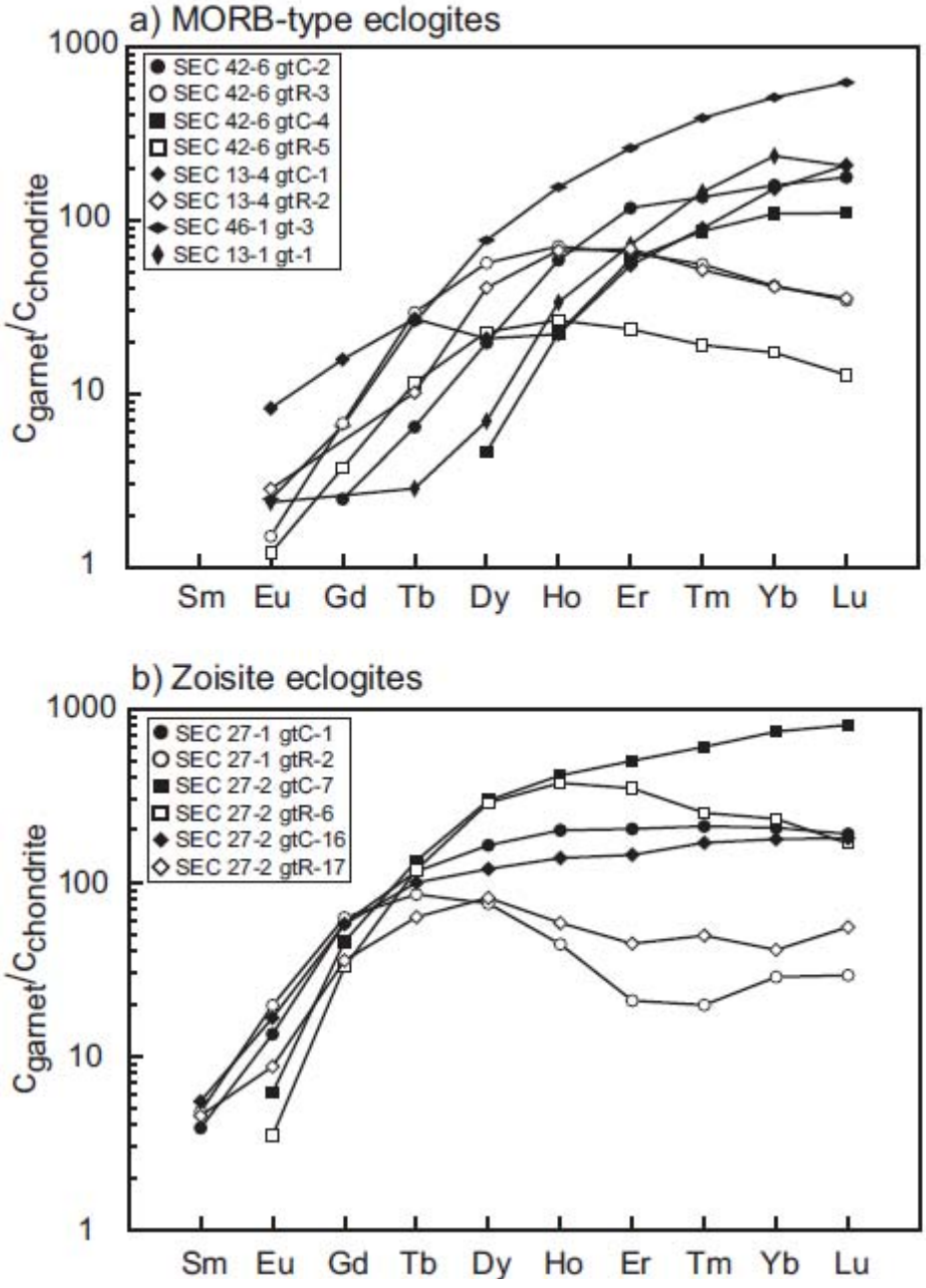

Fig. 3. Lithium concentrations in a) garnet and b) clinopyroxene and amphibole from eclogites of the Raspas Complex. Note that garnet cores tend to be enriched in Li compared to rims. AEC = Amphibole eclogite.

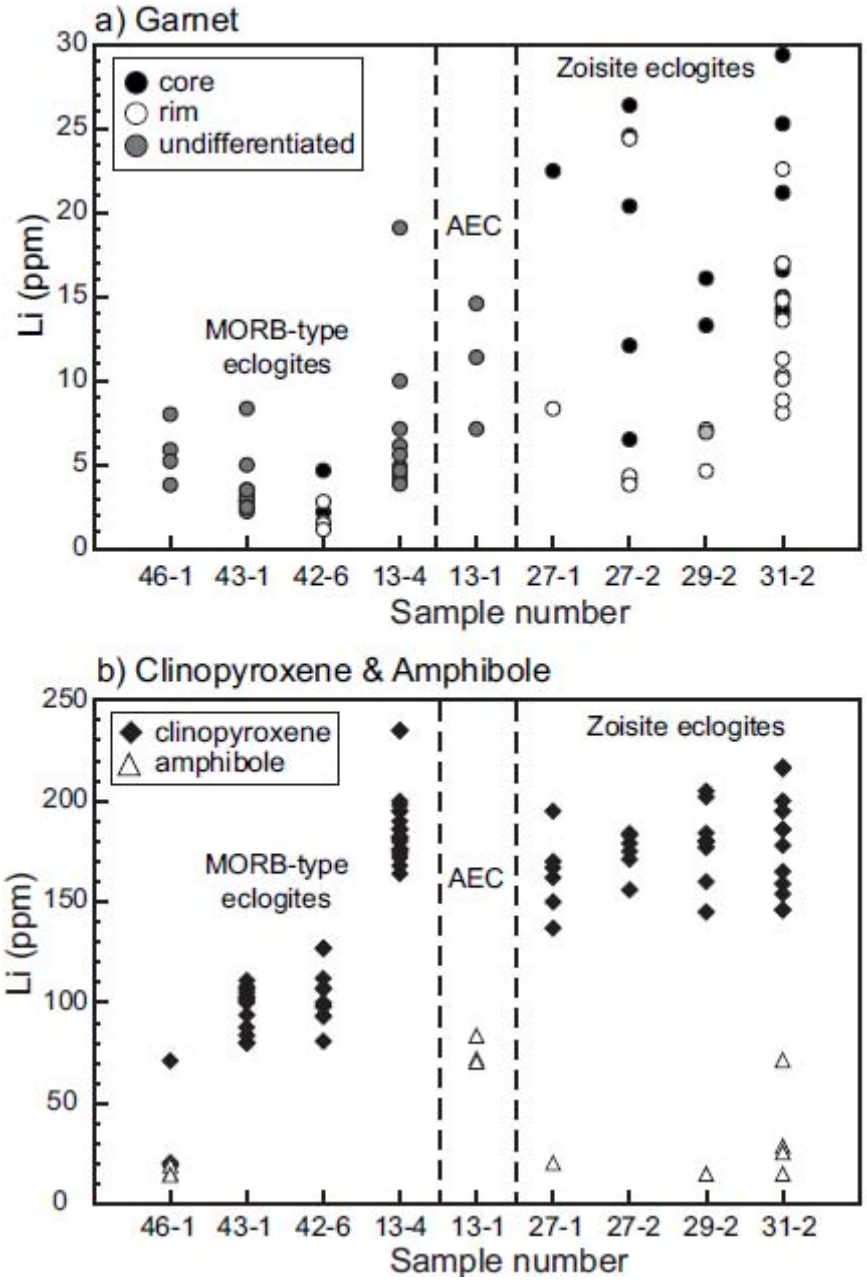

Fig. 4. Back-scattered electron images of two garnet phenocrysts with laser ablation spots and corresponding chemical parameters from a zoisite eclogite of the Raspas Complex. Note the systematic decrease of X_{Fe} from core to rim and the correlated decrease in Li, Sc and Yb concentrations.

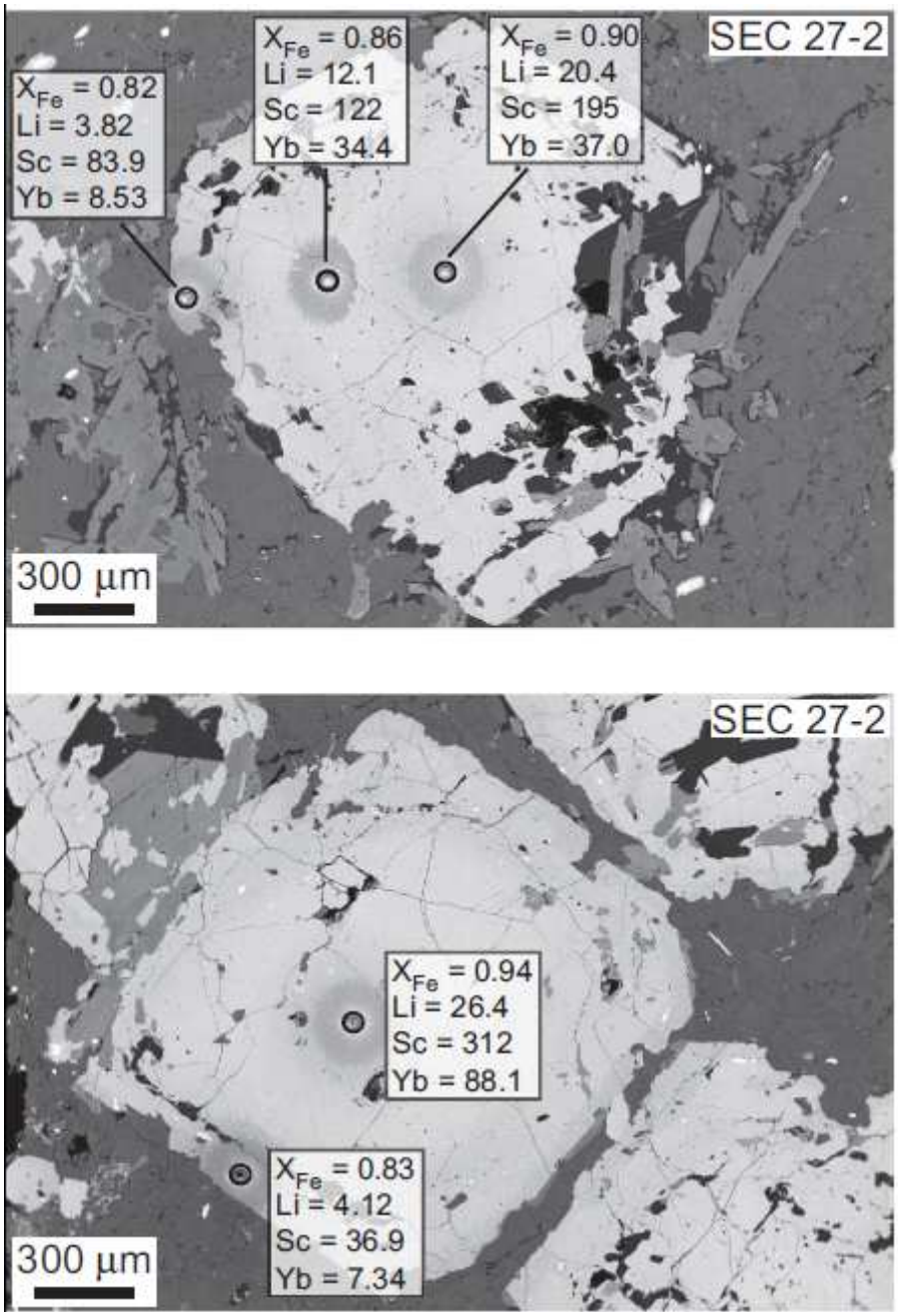

Fig. 5. Oxygen isotope compositions of separated minerals from eclogites of the Raspas Complex (data are from Table 2). a) $\delta^{18}O$ values of garnet, omphacite, amphibole, phengite and zoisite compared to fresh MORB glass (Eiler et al., 2000) and low-temperature (low-T) altered oceanic crust. Data for low-T AOC are from Gregory and Taylor (1981; Oman ophiolite) and Cocker et al. (1982; Macquarie Island ophiolite). b) Oxygen isotopic fractionation between various minerals and garnet plotted versus $\delta^{18}O$ in garnet. The light grey field indicates the approximate limits of O equilibrium fractionation between omphacite and garnet at eclogite-facies conditions after Zheng et al. (2003). The dark grey field shows the limits of zoisite-garnet equilibrium fractionation at 500-700 °C, calculated based on Zheng (1993a, 1993b). Note that, within analytical uncertainty, all omphacite-garnet pairs from the MORB-type eclogites fall into the equilibrium fractionation field, whereas the pairs from the zoisite eclogites do not. Two of the zoisite-garnet pairs are also well outside O isotope equilibrium fractionation.

Fig. 5

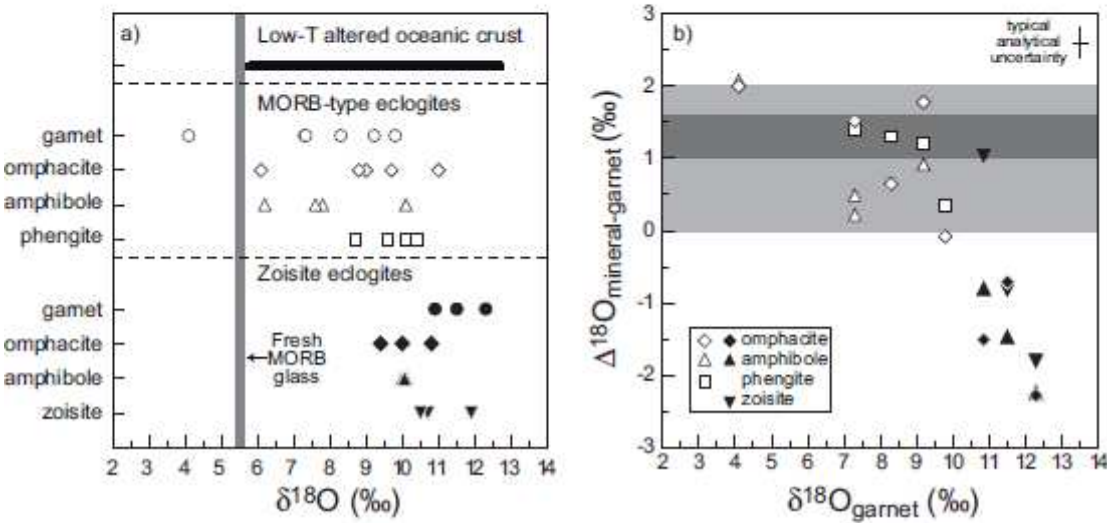

Fig. 6. Sr-Nd isotope diagram of Raspas eclogites and associated rocks (data are from Table 3). The generalized seafloor alteration trend is based on the Sr isotopic composition of seawater at 130 Ma of 0.7073 (Burke et al., 1982) and the typically highly variable $^{87}Sr/^{86}Sr$ ratios at near constant $^{143}Nd/^{144}Nd$ in AOC (Hauff et al., 2003), reflecting the small influence of alteration on the REE (Staudigel et al., 1995). Isotopic compositions of Bulk Silicate Earth (BSE) and Depleted Mantle (DM) at 130 Ma were calculated using the following parameters: For BSE, $^{87}Rb/^{86}Sr$ = 0.0827, $^{87}Sr/^{86}Sr$ = 0.7045 (DePaolo, 1988), $^{147}Sm/^{144}Nd$ = 0.1967 (Peucat et al., 1988), $^{143}Nd/^{144}Nd$ = 0.512638 (Goldstein et al., 1984); for DM, $^{87}Rb/^{86}Sr$ = 0.0460, $^{87}Sr/^{86}Sr$ = 0.7026 (Taylor and McLennan 1985), $^{147}Sm/^{144}Nd$ = 0.2137, $^{143}Nd/^{144}Nd$ = 0.513150 (Peucat et al., 1988). Mixing between an eclogite component, represented by the most depleted MORB-type eclogite sample, and various (meta)sediment-derived components was calculated using the mixing equation: $R_M^X = \frac{R_A^X X_A f + R_B^X X_B (1-f)}{X_A f + X_B (1-f)}$, where R_M^X is an isotope ratio of X in a mixture M of components A and B, X_A and X_B are concentrations of X in A and B, and f is the weight fraction of A in the mixture. Tick marks denote 10% intervals. Symbol size is larger than analytical uncertainty. Field of subducted sediments is based on data from Plank and Langmuir (1998) and Vroon et al. (1995). SAT = Southern Antilles Trench terrigenous sediment, AT = Andaman Trench sediment. S&R 1995 = Snow and Reisberg, 1995.

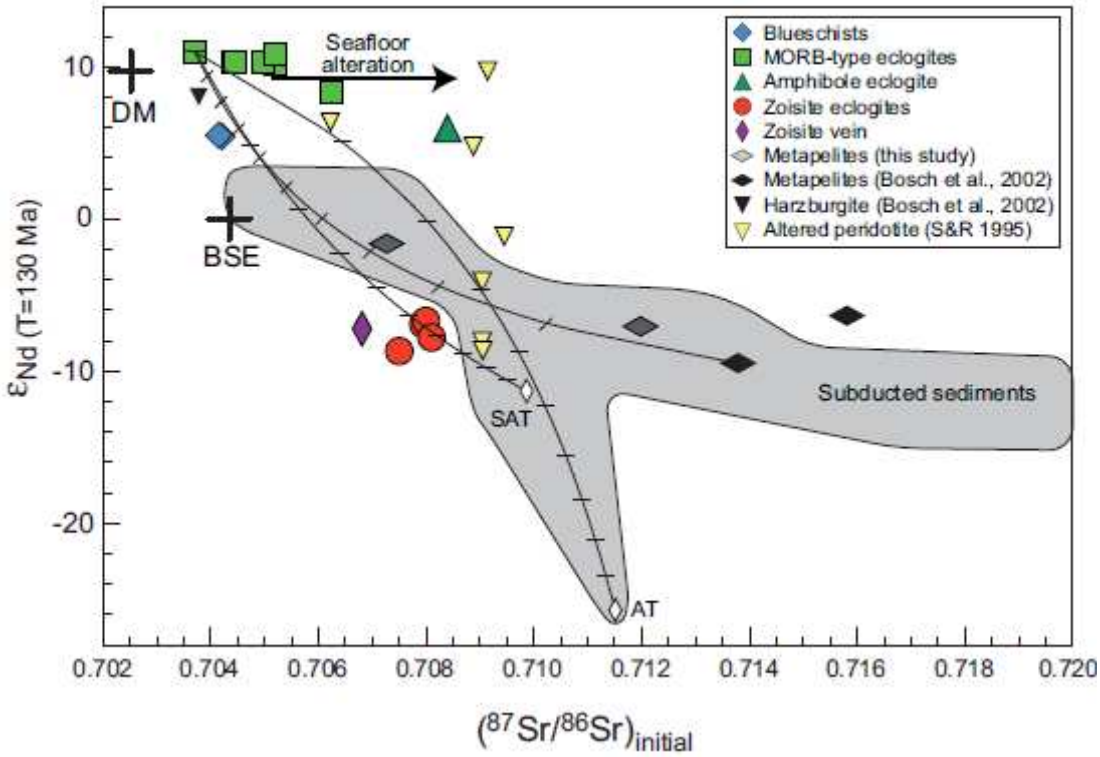

Fig. 7. a) Li/Dy versus Hf/Yb diagram for Raspas eclogites and blueschists. N-MORB, E-MORB and OIB compositions are from Sun and McDonough (1989). AOC composition is the Super Composite from ODP site 801 (Kelley et al., 2003). Note that Li/Dy ratios in many HP metamorphic rocks are significantly higher than in fresh and altered oceanic basalts. Hf/Yb ratios of zoisite eclogites do not necessarily reflect the source compositions due to intense metasomatic effects. b) Li-Sr isotope diagram for the Raspas rocks. Note the lack of correlation for the MORB-type eclogites, suggesting that the low δ^7Li values are not related to seafloor alteration. c) Li isotope compositions of Raspas rocks plotted versus Li concentrations. Compositions of altered oceanic crust (AOC) and highly altered oceanic crust (HAOC) are taken from Marschall et al. (2007b). Small grey dots are orogenic eclogites (Zack et al., 2003; Marschall et al., 2007b). Dehydration curves were modeled in a similar fashion to the Rayleigh distillation models from Zack et al. (2003), using a bulk solid-liquid partition coefficient of 0.15 for Li and values of 1.007 and 1.003 for the Li isotope fractionation factor, defined as $(^7Li/^6Li)_{fluid}/(^7Li/^6Li)_{rock}$, for temperatures of 200 °C (dashed lines) and 600 °C (solid lines), respectively (Wunder et al., 2006). The concentration of Li in the remaining solid after dehydration was calculated using the equation $c_s = c_o(1-F)^{\frac{1}{D-1}}$, where c_s is the concentration of Li in the remaining solid, c_o is the original Li concentration, D is the bulk distribution coefficient, and F is the proportion of fluid removed. A water content of 6 wt.% H_2O was assumed for the hydrated basalt. δ^7Li in the remaining dehydrated rock was calculated as $\delta^7 Li_{rock} = \left(\delta^7 Li_o + 1000\right) f^{(\alpha-1)} - 1000$, where α is the Li isotope fractionation factor and f is the fraction of Li remaining in the rock ($f = c_s/c_o$). The dehydration models are not able to explain any of the low-δ^7Li, high-Li data of the HP metamorphic rocks. d) Li-N isotope diagram for the Raspas rocks. N isotope data are from Halama et al. (2010). Linear correlations with correlation coefficient R^2 are shown for the MORB-type eclogites and the blueschists. The apparent negative correlations cannot be due to seafloor alteration, which would produce a trend towards more positive δ^7Li values. Hence, they are interpreted to reflect the effects of localized metasomatism.

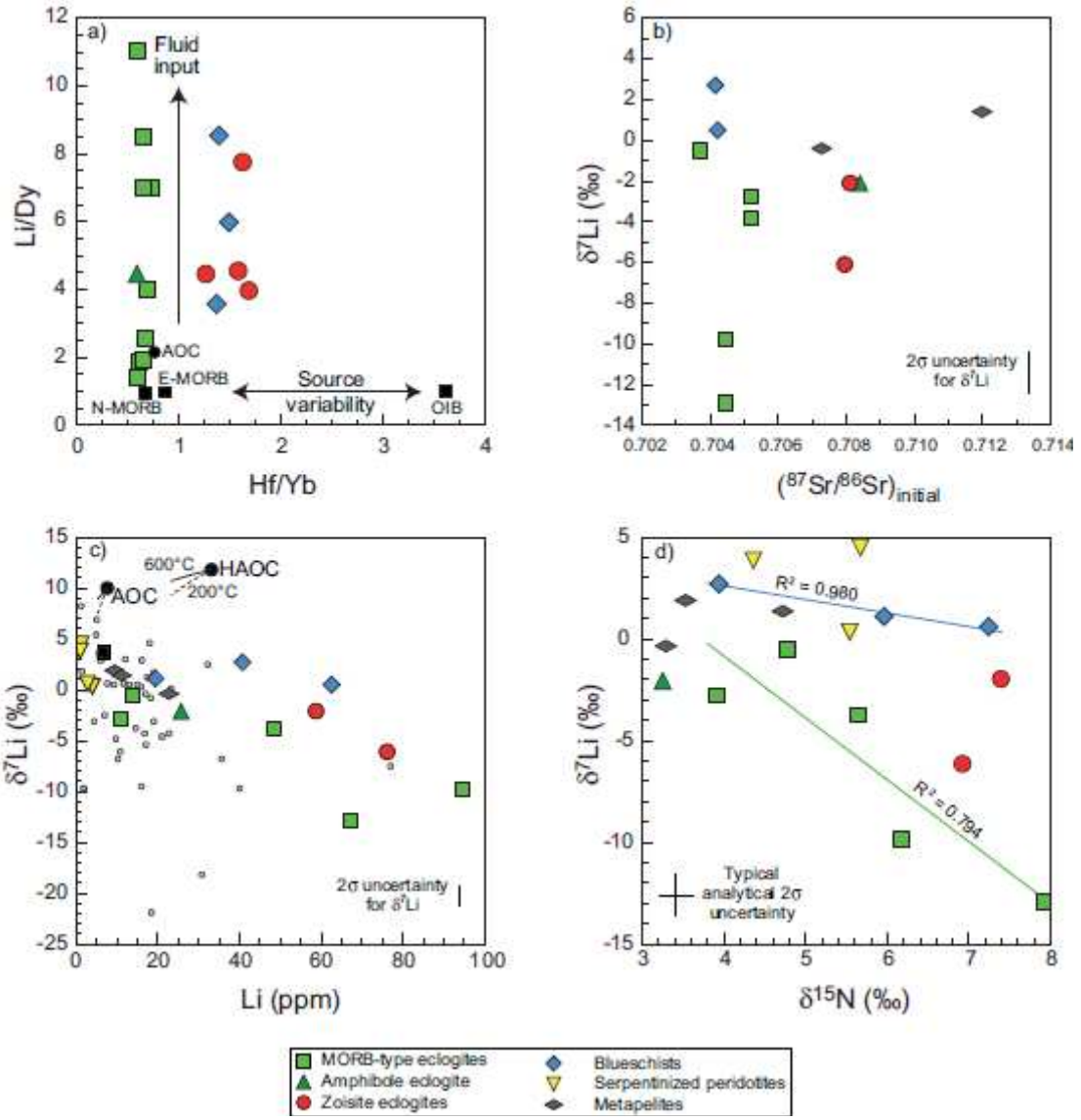

Table 1. Representative LA-ICP-MS analyses of garnets from Raspas eclogites.

	SEC	SEC	SEC	SEC	SEC	SEC	SEC	SEC	SEC	SEC	SEC	SEC	
Sample	46-1	42-6	42-6	13-4	13-4	13-1	27-2	27-2	27-2	27-2	29-2	29-2	DL
Rock type	MTEC	MTEC	MTEC	MTEC	MTEC	AEC	ZEC	ZEC	ZEC	ZEC	ZEC	ZEC	
Mineral	Grt	Grt	Grt	Grt	Grt	Grt	Grt	Grt	Grt	Grt	Grt	Grt	
Comment		core	rim	core	rim		core	rim	core	rim	core	rim	
In µg/g:													
Li	5.90	2.20	1.49	3.98	4.86	14.6	24.6	24.4	26.4	4.12	16.1	7.12	0.90
Sc	69.1	100	60.0	96.6	84.1	156	602	70.2	312	36.9	72.0	55.7	0.58
Ti	789	406	361	532	406	754	656	746	787	415	821	500	3.15
Cr	85.8	256	163	142	49.2	167	50.4	55.4	57.3	119	104	93.4	6.54
Sr	0.588	<0.05	<0.04	0.093	0.136	0.963	0.120	<0.06	<0.06	<0.06	<0.09	<0.08	0.07
Y	304	120	130	57.9	147	61.0	670	734	485	30.8	122	24.8	0.07
Zr	6.02	1.05	1.10	0.389	1.75	1.47	0.672	1.90	1.16	1.31	2.87	1.90	0.14
Sm	<0.29	<0.69	<0.43	<0.55	<0.39	<0.51	<0.97	<0.46	1.60	0.357	1.66	<0.53	0.51
Eu	0.182	<0.11	0.111	0.606	0.208	0.174	0.452	0.256	0.544	0.095	0.805	<0.12	0.12
Gd	1.69	0.641	1.75	4.08	<0.51	<0.59	11.8	8.41	14.5	1.28	10.7	0.786	0.50
Tb	1.22	0.305	1.39	1.28	0.481	0.135	6.31	5.60	6.98	0.470	3.35	0.252	0.08
Dy	24.6	6.32	18.2	6.68	13.1	2.24	95.3	92.4	82.5	3.17	21.5	3.28	0.35
Ho	11.1	4.22	5.06	1.58	4.79	2.41	29.6	26.8	21.4	0.897	4.62	0.936	0.08
Er	54.4	24.6	13.6	11.5	14.3	15.1	105	72.9	64.9	4.36	14.9	3.35	0.26
Tm	12.5	4.38	1.80	2.90	1.67	4.69	19.5	8.13	10.9	1.04	2.17	0.678	0.08
Yb	106	33.1	8.73	31.6	8.64	48.8	154	48.5	88.1	7.34	17.1	6.54	0.42
Lu	19.9	5.67	1.11	6.66	1.14	6.58	25.9	5.38	15.1	1.33	2.56	1.10	0.09

DL = Detection limit, AVG = Average, STDEV = Standard deviation, RSD = Relative standard deviation;
MTEC = MORB-type eclogite; AEC = Amphibole eclogite; ZEC = Zoisite eclogite;
Be, B, Ni, Rb, Nb, Cs, Ba, La, Ce, Pr, Nd, Hf, Ta, Pb, Th and U were mostly below or near the detection limits and are therefore not shown.

Table 2. Oxygen isotope data of mineral separates from Raspas HP metamorphic rocks.

Sample	Rock type	Mineral	$\delta^{18}O$
SEC 16-1	blueschist	garnet	8.4
		glaucophane	9.3
		green amphibole	9.7
		phengite	10.2
SEC 42-6	MORB-type eclogite	garnet	9.8
		omphacite	9.7
		phengite	10.1
SEC 43-1	MORB-type eclogite	garnet	8.3
		omphacite	9.0
		phengite	9.6
SEC 44-1	MORB-type eclogite	garnet	9.2
		omphacite	11.0
		amphibole	10.1
		phengite	10.4
SEC 46-1	MORB-type eclogite	garnet	4.1
		omphacite	6.1
		amphibole	6.2
SEC 47-1	MORB-type eclogite	garnet	7.3
		omphacite	8.8
		amphibole	7.8
		phengite	8.7
SEC 13-1	amphibole eclogite	garnet	7.3
		amphibole	7.6
SEC 29-2	zoisite eclogite	garnet	10.9
		omphacite	9.4
		amphibole	10.1
		zoisite	11.9
SEC 31-2-2	zoisite eclogite	garnet	11.5
		omphacite	10.8
		amphibole	10.0
		zoisite	10.7
SEC 31-2-3	zoisite eclogite	garnet	12.3
		omphacite	10.0
		amphibole	10.1
		zoisite	10.5
SEC 31-2-1	zoisite vein	zoisite	12.1
		zoisite	11.8

Table 3. Sr-Nd isotope data of HP metamorphic rocks from the Raspas Complex.

Sample	Rock type	Rb (ppm)	Sr (ppm)	$(^{87}Sr/^{86}Sr)_m$	$^{87}Rb/^{86}Sr$	$(^{87}Sr/^{86}Sr)_i$	Sm (ppm)	Nd (ppm)	$(^{143}Nd/^{144}Nd)_m$	$^{147}Sm/^{144}Nd$	$(^{143}Nd/^{144}Nd)_i$	$\varepsilon Nd_{(T=130\ Ma)}$	εNd_0
SEC 16-1	blueschist	28.2	329	0.704668 (5)	0.248	0.704210	7.35	31.2	0.512870 (3)	0.142	0.512750	5.4	4.5
SEC 17-3	blueschist	7.11	376	0.704253 (4)	0.055	0.704151	6.61	27.7	0.512876 (3)	0.144	0.512753	5.5	4.6
SEC 13-4	MTEC	0.04	77.4	0.704431 (5)	0.001	0.704429	5.00	13.2	0.513197 (3)	0.229	0.513002	10.4	10.9
SEC 42-6	MTEC	4.38	76.7	0.706562 (4)	0.165	0.706257	5.36	15.5	0.513072 (2)	0.208	0.512895	8.3	8.5
SEC 43-1	MTEC	15.33	92.5	0.706091 (5)	0.479	0.705205	4.03	11.5	0.513174 (2)	0.210	0.512995	10.2	10.4
SEC 43-3	MTEC	1.06	77.0	0.703781 (5)	0.040	0.703708	4.38	12.6	0.513214 (3)	0.210	0.513035	11.0	11.2
SEC 44-1	MTEC	13.06	66.8	0.706034 (5)	0.566	0.704988	4.23	11.9	0.513182 (3)	0.214	0.513000	10.3	10.6
SEC 46-1	MTEC	0.53	31.6	0.705275 (5)	0.048	0.705186	5.11	13.9	0.513213 (2)	0.222	0.513024	10.8	11.2
SEC 47-1	MTEC	12.7	103	0.705102 (4)	0.356	0.704444	4.54	12.4	0.513189 (3)	0.221	0.513001	10.3	10.8
SEC 13-1	AEC	0.60	17.4	0.708577 (5)	0.100	0.708393	0.84	2.99	0.512921 (4)	0.170	0.512776	6.0	5.5
SEC 27-1	ZEC	1.33	343	0.707522 (5)	0.011	0.707501	15.7	82.5	0.512123 (3)	0.115	0.512026	-8.7	-10.0
SEC 29-2	ZEC	1.61	351	0.707969 (5)	0.013	0.707945	11.1	55.4	0.512219 (3)	0.120	0.512117	-6.9	-8.2
SEC 31-2-2	ZEC	1.53	588	0.708010 (4)	0.008	0.707996	14.6	72.5	0.512231 (2)	0.121	0.512128	-6.7	-7.9
SEC 31-2-3	ZEC	1.40	255	0.708131 (5)	0.016	0.708101	14.1	70.7	0.512174 (3)	0.120	0.512072	-7.8	-9.1
SEC 31-2-1	zoisite vein	19.4	3550	0.706839 (5)	0.016	0.706810	24.3	108.6	0.512216 (2)	0.135	0.512101	-7.2	-8.2
SEC 32-2	metapelite	29.5	37.3	0.716214 (5)	2.291	0.711980	2.45	13.0	0.512206 (3)	0.114	0.512109	-7.1	-8.4
SEC 42-3	metapelite	64.6	129	0.709950 (5)	1.451	0.707268	5.03	20.7	0.512513 (3)	0.146	0.512388	-1.6	-2.4

MTEC = MORB-type eclogite, AEC = amphibole eclogite, ZEC = zoisite eclogite
m = measured; numbers in parentheses give the internal error of the measurement referring to the last significant digit
i = initial; initial Sr and Nd isotopic compositions were calculated for T = 130 Ma
Rb, Sr, Sm and Nd concentration data are from John et al. (2010) and Halama et al. (2010)

Table 4. Lithium concentrations, Li isotope compositions, Li/Dy ratios and Hf/Yb ratios of metamorphic rocks from the Raspas Complex.

Sample	Rock type	Material	Li (ppm)*	δ^7Li	Li/Dy**	Hf/Yb**
SEC 15-2	blueschist	WR	19.4	1.1	3.57	1.37
SEC 16-1	blueschist	WR	62.5	0.3	8.54	1.39
SEC 16-1 REPL				0.8		
SEC 16-1 AVG				**0.5**		
SEC 16-1 Grt		Grt	6.25	3.7		
SEC 16-1 Phengite		Phe	28.6	3.2		
SEC 16-1 Gln		Gln	89.6	-0.4		
SEC 17-3	blueschist	WR	40.7	2.7	5.98	1.49
SEC 13-4	MORB-type eclogite	WR	94.4	-9.8	11.04	0.59
SEC 42-6	MORB-type eclogite	WR	35.2		3.98	0.69
SEC 43-1	MORB-type eclogite	WR	48.5	-3.5	6.98	0.72
SEC 43-1 REPL			48.5	-4.0		
SEC 43-1 AVG				**-3.8**		
SEC 43-1 Grt		Grt	2.87#	-0.8		
SEC 43-1 Omp		Omp	77.7#	-3.9		
SEC 43-1 Omp REPL			82.4#	-4.1		
SEC 43-1 Omp AVG			**80.1**	**-4.0**		
SEC 43-3	MORB-type eclogite	WR	13.8	-0.5	1.89	0.62
SEC 44-1	MORB-type eclogite	WR	51.4		6.99	0.64
SEC 46-1	MORB-type eclogite	WR	11.0	-2.8	1.40	0.59
SEC 46-2	MORB-type eclogite	WR	13.3		1.92	0.64
SEC 47-1	MORB-type eclogite	WR	67.3	-12.9	8.50	0.65
SEC 50-1	retrogressed eclogite	WR	20.3		2.53	0.66
SEC 13-1	amphibole eclogite	WR	25.7	-2.1	4.46	0.59
SEC 13-1 Grt		Grt	5.17#	-3.0		
SEC 13-1 Cam		Cam	59.5#	-0.7		
SEC 27-1	zoisite eclogite	WR	65.3		4.55	1.58
SEC 29-2	zoisite eclogite	WR	76.1	-6.1	7.76	1.62
SEC 31-2-2	zoisite eclogite	WR	45.6		3.97	1.68
SEC 31-2-3	zoisite eclogite	WR	58.7	-2.1	4.46	1.26
SEC 31-2-1	zoisite vein	WR	0.92	18.3	0.12	0.35
SEC 26-3	serpentinitized peridotite	WR	0.84		6.76	0.12
SEC 26-9	serpentinitized peridotite	WR	3.96	0.4	10.83	0.24
SEC 26-9 REPL				0.2		
SEC 26-9 AVG				**0.3**		
SEC 34-1	serpentinitized peridotite	WR	1.18	4.5	5.82	0.17
SEC 35-2	serpentinitized peridotite	WR	0.99	3.8	3.72	1.17
SEC 36-2	serpentinitized peridotite	WR	1.03		16.87	0.19
SEC 40-1	serpentinitized peridotite	WR	2.76	0.5	20.59	0.08
SEC 40-1 REPL				0.6		
SEC 40-1 AVG				**0.6**		
SEC 32-2	metapelite	WR	11.1	1.4	7.74	9.24
SEC 42-3	metapelite	WR	22.7	-0.4	3.94	0.88
SEC 47-4	metapelite	WR	9.37	1.9	1.97	2.38

WR = Whole rock; Grt = Garnet; Omp = Omphacite; Phe = Phengite; Gln = Glaucophane; Cam = Ca-rich clinoamphibole;
REPL = Replicate analysis; AVG = Average
* Li concentrations measured by solution ICP-MS at the University of Kiel
** Li/Dy and Hf/Yb ratios based on data from John et al. (2010) and Halama et al. (2010)

[#] Li concentrations measured by voltage comparison between sample and L-SVEC solutions, 1σ uncertainty ≤ 10% (Teng et al., 2007)